

This article was downloaded by:

On: 25 January 2011

Access details: *Access Details: Free Access*

Publisher *Taylor & Francis*

Informa Ltd Registered in England and Wales Registered Number: 1072954 Registered office: Mortimer House, 37-41 Mortimer Street, London W1T 3JH, UK



Liquid Crystals

Publication details, including instructions for authors and subscription information:

<http://www.informaworld.com/smpp/title~content=t713926090>

Study of relaxations in cholesteric liquid crystals after reduction of an electric field

James E. Anderson; Philip Watson; Philip J. Bos

Online publication date: 06 August 2010

To cite this Article Anderson, James E. , Watson, Philip and Bos, Philip J.(2001) 'Study of relaxations in cholesteric liquid crystals after reduction of an electric field', *Liquid Crystals*, 28: 6, 945 – 968

To link to this Article: DOI: 10.1080/02678290110035187

URL: <http://dx.doi.org/10.1080/02678290110035187>

PLEASE SCROLL DOWN FOR ARTICLE

Full terms and conditions of use: <http://www.informaworld.com/terms-and-conditions-of-access.pdf>

This article may be used for research, teaching and private study purposes. Any substantial or systematic reproduction, re-distribution, re-selling, loan or sub-licensing, systematic supply or distribution in any form to anyone is expressly forbidden.

The publisher does not give any warranty express or implied or make any representation that the contents will be complete or accurate or up to date. The accuracy of any instructions, formulae and drug doses should be independently verified with primary sources. The publisher shall not be liable for any loss, actions, claims, proceedings, demand or costs or damages whatsoever or howsoever caused arising directly or indirectly in connection with or arising out of the use of this material.

Study of relaxations in cholesteric liquid crystals after reduction of an electric field

JAMES E. ANDERSON*, PHILIP WATSON and PHILIP J. BOS

Liquid Crystal Institute and Chemical Physics Interdisciplinary Program,
 Kent State University, Kent, Ohio 44242, USA

(Received 7 August 2000; accepted 30 August 2000)

It is well known that, upon reduction of an applied electric field, cholesteric systems transform to their equilibrium state through a ‘transient planar’ state. However, the detailed description of this transformation, as a function of bias voltage, has not been known. In this paper we study a cholesteric sample having a thickness of $15\ \mu\text{m}$ and a pitch of $5.36\ \mu\text{m}$ using both experimental and numerical simulation. We show the details of the director field dynamics as these systems transform from the high field homeotropic state to the equilibrium state, as a function of voltage. From this understanding we will suggest improvements for increasing the speed of these transitions.

1. Introduction

Cholesteric liquid crystal (LC) systems are LC systems in which the LC director rotates in space about some axis [1]; this spatial periodicity leads to Bragg reflection [1]. The peak wavelength of this reflection is given by $\lambda_{\text{peak}} = \langle n \rangle P$, where $\langle n \rangle$ is the average index of refraction and P is the pitch of the system, defined as the spatial distance over which the director rotates 360 degrees [1]. Earlier work has studied the dynamics of these systems [2–4], however none of these works showed detailed director dynamics of the systems when a field large enough to drive the system into the homeotropic (H) state, a state in which all the directors are aligned perpendicular (or nearly perpendicular) to the substrates, is reduced. More recently, we have shown the director field for these systems when the electric field was completely removed [5]. In this paper we show the detailed response of a cholesteric LC director field as the voltage is reduced from a high value to some non-zero lower value.

2. Background

It has been shown experimentally that, upon reduction of the applied field to a bias voltage, for certain bias voltages the system first transforms to a ‘transient planar’ (TP) state [4]. This state is characterized by the fact

that all (or nearly all) the local helical axes are aligned perpendicular to the substrates. The pitch in the TP state can be approximated by $P^* = P_0 K_{33}/K_{22}$, where P_0 is the intrinsic pitch of the system, and K_{22} and K_{33} are the twist and bend elastic constants, respectively [2]. However, the mechanics of the transformation from the TP state to the equilibrium state—either the planar (P) state which is similar to the TP state, but which now has pitch P_0 , or the focal-conic (FC) state, which has (on average) the helical axes lying parallel to the substrate plane—are not known. It is the aim of this paper to elucidate the mechanisms and director structures involved in the transformations that occur when an applied field large enough to form the homeotropic state is reduced to various bias voltages.

3. Computer simulation method

To simulate the director structure numerically, we implemented a two-dimensional program based on the Frank–Oseen free energy density given in equation (1) [1]:

$$f_g = \frac{1}{2} K_{11} (\nabla \cdot \mathbf{n})^2 + \frac{1}{2} K_{22} (\mathbf{n} \cdot \nabla \times \mathbf{n} + q_0)^2 + \frac{1}{2} K_{33} |\mathbf{n} \times \nabla \times \mathbf{n}|^2 - \frac{1}{2} \mathbf{D} \cdot \mathbf{E} \quad (1)$$

*Author for correspondence; e-mail: janderson@hanaoh.com

Here \mathbf{n} is the unit vector direction, K_{11} , K_{22} , K_{33} are the splay, twist and bend elastic constants respectively, q_0 is the chiral wavenumber ($= 2\pi/P_0$), \mathbf{D} is the electric displacement and \mathbf{E} is the electric field. We used the relaxation method, with the update formula given in equation (2), which can be derived from setting the viscous torque equal to the elastic torque [6–9]:

$$n_i^{\text{new}} = n_i^{\text{old}} - \frac{\Delta t}{\gamma_1} [f_g]_{n_i}, \quad i = x, y, z. \quad (2)$$

Here Δt is the numerical time step used in simulation, γ_1 is the rotational viscosity of the material, n_i^{new} denotes the new value of the component of the director, n_i^{old} denotes the value at the previous time step and $[f_g]_{n_i}$ is the functional derivative, given in equation (3):

$$[f_g]_{n_i} \equiv \frac{\partial f_g}{\partial n_i} - \frac{d}{dx} \left[\frac{\partial f_g}{\partial (dn_i/dx)} \right] - \frac{d}{dy} \left[\frac{\partial f_g}{\partial (dn_i/dy)} \right]. \quad (3)$$

To determine the new voltage profile, we used a direct method based on the fact that when Gauss's law ($\nabla \cdot \mathbf{D} = 0$) is discretized, an equation linear in the values of the discretized voltage results [9]. This equation can then be solved for the new value of the voltage at the current grid point in terms of the values at the surrounding grid points.

In order to simulate the transition from the homeotropic state, we had to introduce some small amount of random noise to the initial director configuration. If the director was assumed to be exactly homeotropic ($n_x = 0$, $n_y = 0$, $n_z = 1$), then the program will not move the director, as there is no net torque. To overcome this, we set n_x and n_y to be a random number between -0.5 and $+0.5$ in the bulk. We then used the unit length of the director to determine n_z , $n_z = \sqrt{1 - n_x^2 - n_y^2}$. In order to compare each bias voltage calculation with each other, we generated one starting configuration and used that for all calculations.

The physical size of the calculation was assumed to be $25 \mu\text{m} \times 15 \mu\text{m}$ in the x and z directions, respectively with 208×125 grid points. This yields a square grid with spacing $120 \text{ nm} \times 120 \text{ nm}$. The z dimension was chosen simply to be the same as the cell gap. The x dimension was chosen to give the minimum free energy during the initiation of the undulation distortion. To determine this, we calculated the total free energy of the configuration just after the undulation started; this was calculated by integrating equation (1). We then changed the lateral dimension to determine the value that gave the lowest free energy. We also measured the wavelength of the distortion and found it to be $15.6 \mu\text{m}$. The simulation

had two full wavelengths, so the simulated wavelength on minimum energy was $12.5 \mu\text{m}$. The slight difference between the simulation and experiment is probably related to imprecise measurement of thickness and pitch (see next section).

The boundary conditions in the x direction were periodic, which assumes the director configuration calculated is one period in a repeated structure. To achieve this boundary condition, we set the $x = 0$ boundary to be the same as the $x = 207$ boundary; derivatives are then calculated as a loop, so that the derivative at $x = 0$ uses the directors at $x = 1$ and $x = 206$ [9].

This simulation method does not allow for a variable scalar order parameter, which is required for defects to form. We found, however, that at no time during the calculation did the free energy density become large enough for a defect to form [5].

4. Cholesteric system under study

In this study we chose to use a long pitch cholesteric LC sandwiched between two glass plates such that the thickness to pitch ratio (d/P) was 2.8. The same sample has been used in other reports [5, 10, 11]. The pitch was measured by the Grandjean–Cano method to be $5.36 \pm 0.05 \mu\text{m}$; the thickness was measured by an interference method to be $15.0 \pm 0.2 \mu\text{m}$. The long pitch, coupled with the low d/P ratio, causes this system to move through the transition slowly, taking around 1 s to complete the transition. In this way we were able to get clear and accurate experimental results.

The LC was a mixture of 97% ZLI-4792 and 3% CB15, a chiral agent used to induce the twist. The cells used in this study employed ITO coated soda lime glass coated with Dupont 2555 polyimide. The polyimide was rubbed to give a pretilt of roughly 5 degrees. The two glass substrates were aligned such that the rubbing directions were anti-parallel.

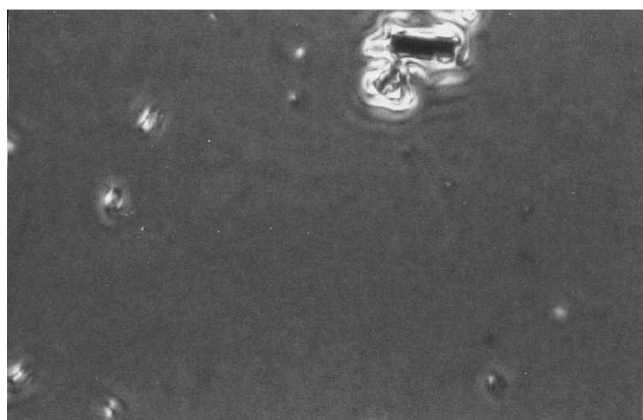
It has been theoretically suggested that the transient planar pitch is given by $P^* = P_0 K_{33}/K_{22}$ [2]. Because the percentage of chiral dopant is so low in this system, we can use parameter values of ZLI-4792 for calculations. For ZLI-4792, the ratio $K_{33}/K_{22} = 2.815$ [12]. We therefore expect the TP state to have a pitch of roughly $15.1 \mu\text{m}$, which would imply only one full twist in this state. The P state, on the other hand should have three full twists.

5. Experimental

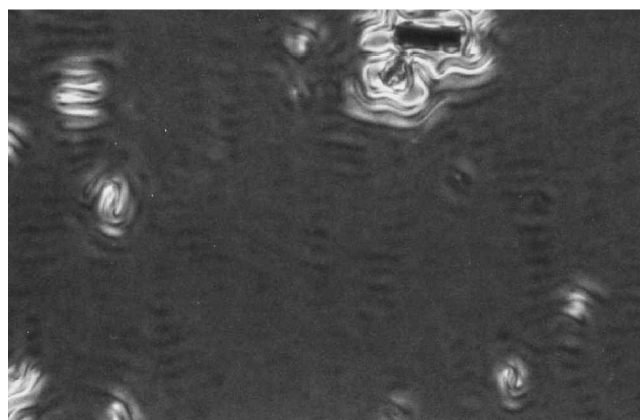
To observe the dynamics of this system, two experimental techniques were used. We measured the capacitance as a function of time and took photomicrographs at various times during the transition using a

flash-lamp system. Measuring the capacitance was accomplished by connecting a known capacitance, C_0 , in series with the sample and measuring the voltage across the known capacitance as a function of time [13]. The

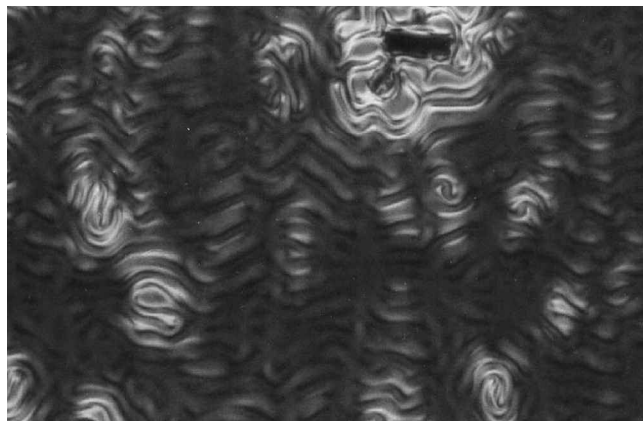
equation for the capacitance of the sample is derived in equation (4), which is based on setting the charge on the plates equal. We ensured $C_0 \gg C_{LC}$ so that the voltage across the LC sample could be assumed to be the applied



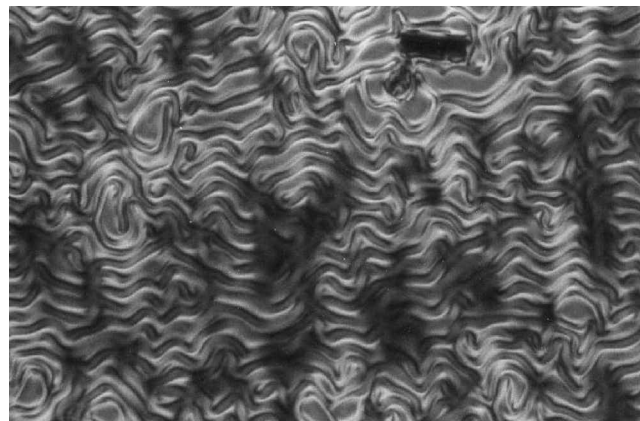
(a)



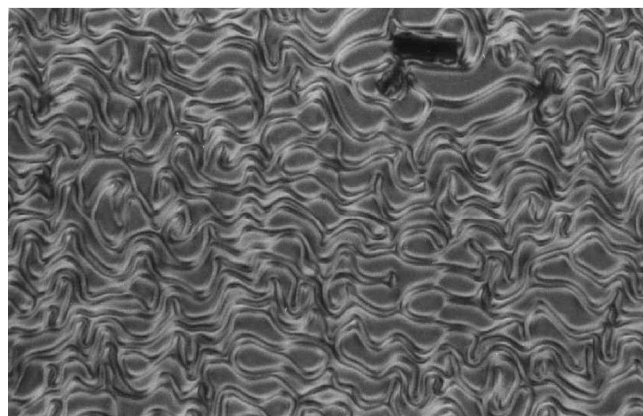
(b)



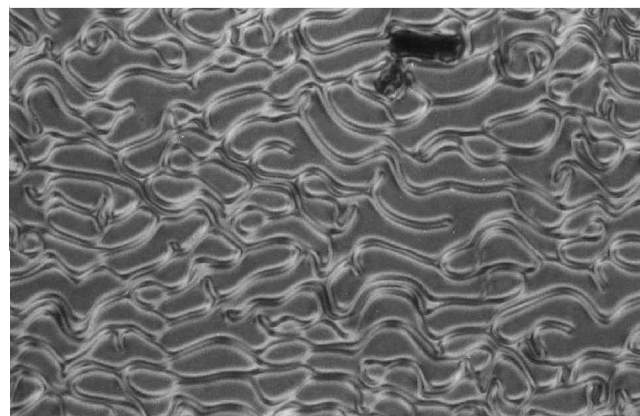
(c)



(d)



(e)



(f)

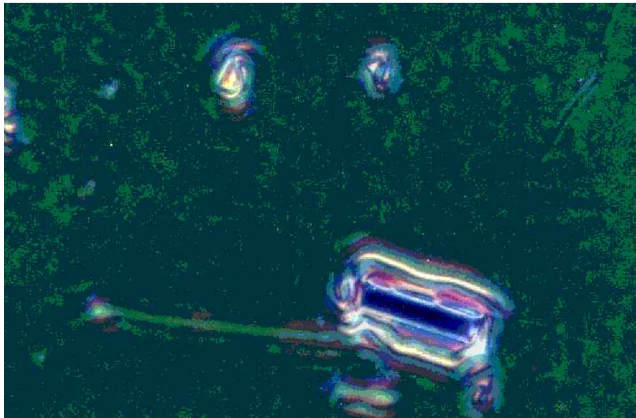
Figure 1. Microphotographs of the transition from the high voltage to bias voltage. Voltages and times are: (a) 0 V 200 ms, (b) 0 V 300 ms, (c) 0 V 400 ms, (d) 0 V 500 ms, (e) 0 V 700 ms, (f) 0 V 1000 ms, (g) 2 V 200 ms, (h) 2 V 300 ms, (i) 2 V 400 ms, (j) 2 V 500 ms, (k) 2 V 700 ms, (l) 2 V 1000 ms, (m) 4 V 200 ms, (n) 4 V 300 ms, (o) 4 V 400 ms, (p) 4.5 V 200 ms, (q) 4.5 V 300 ms, (r) 4.5 V 400 ms, (s) 5 V 200 ms, (t) 5 V 300 ms, (u) 5 V 400 ms, (v) 5 V 500 ms, (w) 5 V 700 ms, (x) 5 V 1000 ms.

voltage. In our experiment, the value of C_0 was $0.455 \mu\text{F}$.

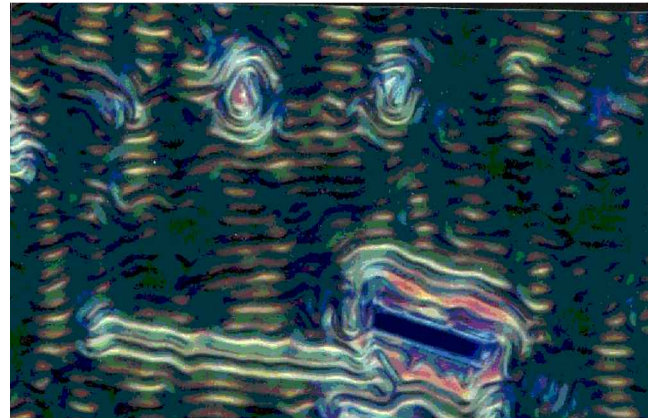
$$\frac{V_{\text{measured}}}{V_{\text{applied}}} = \frac{C_{\text{total}}}{C_0}, \quad \frac{1}{C_{\text{total}}} = \frac{1}{C_0} + \frac{1}{C_{\text{LC}}}, \quad (4)$$

$$C_{\text{total}} = \frac{C_0 C_{\text{LC}}}{C_0 + C_{\text{LC}}} \cong C_{\text{LC}}, \quad \Rightarrow C_{\text{LC}} \cong C_0 \frac{V_{\text{measured}}}{V_{\text{applied}}}.$$

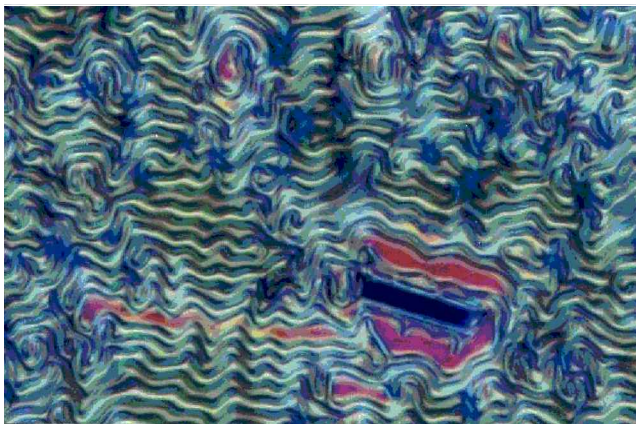
In the second experiment, we used a Nikon Optiphot 2 polarizing microscope with a Leitz 35 mm camera, a Xe flash lamp and electronic components to obtain photomicrographs of the transition with a temporal resolution of roughly $20 \mu\text{s}$. The standard Nikon microscope light source was replaced by an Oriel series 6427 Xe flash-lamp with 5 J maximum output and a full width half



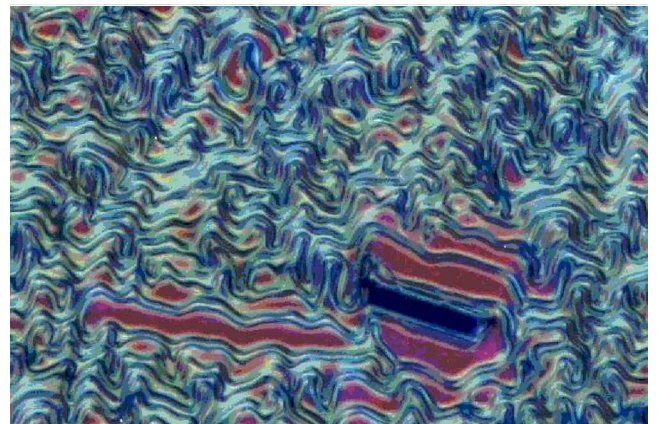
(g)



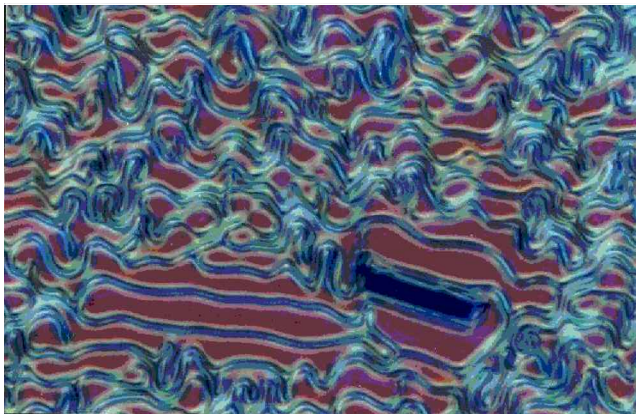
(h)



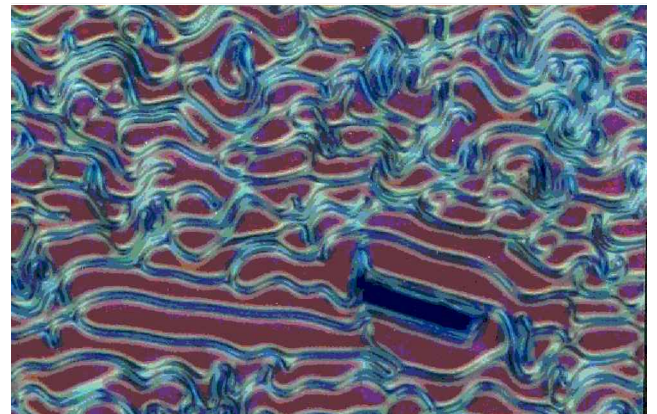
(i)



(j)



(k)



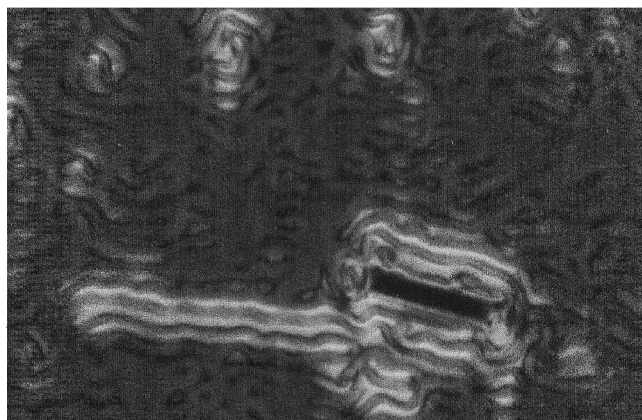
(l)

Figure 1. (Continued).

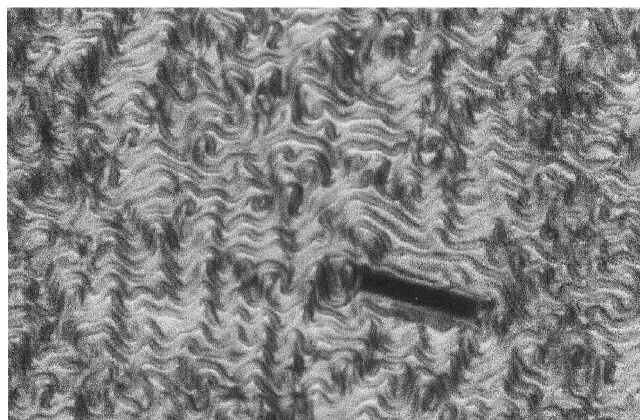
maximum of $9\ \mu\text{s}$. To obtain high resolution pictures, we used 35 mm Kodak Max 800 DIN film at $200\times$ optical magnification.

The voltage applied to the sample in both experimental set-ups was a 1 kHz square wave generated by an

Analogic Model 2020 polynomial waveform synthesizer. The voltage was applied for 5 s in the homeotropic state (40.5 V) to ensure full alignment and then reduced to the bias level (0 – 5 V) for 5 s, during which time the experimental data were taken.



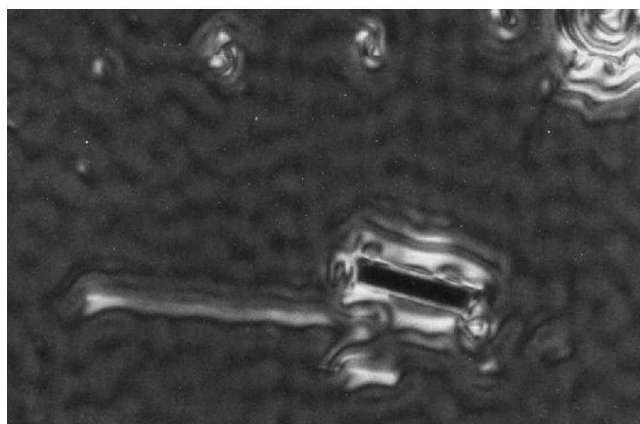
(m)



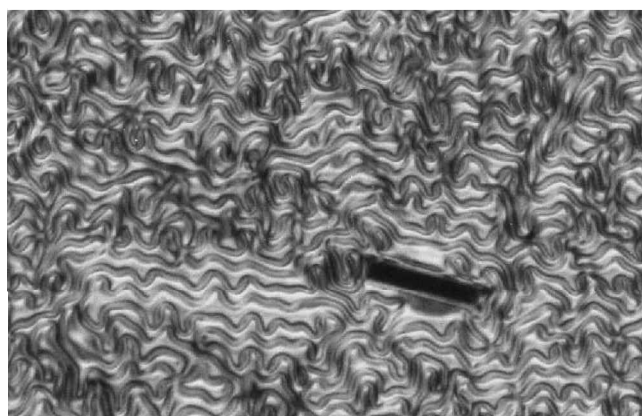
(n)



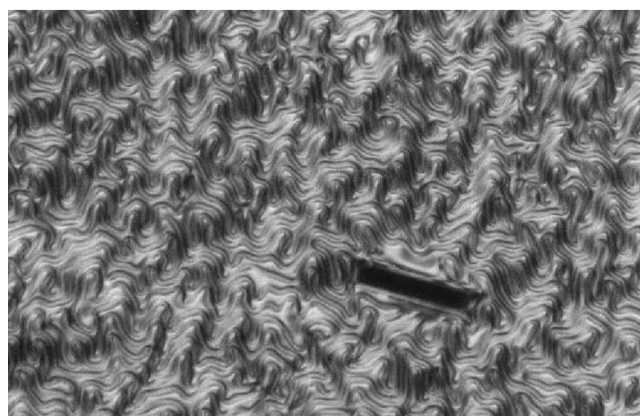
(o)



(p)



(q)



(r)

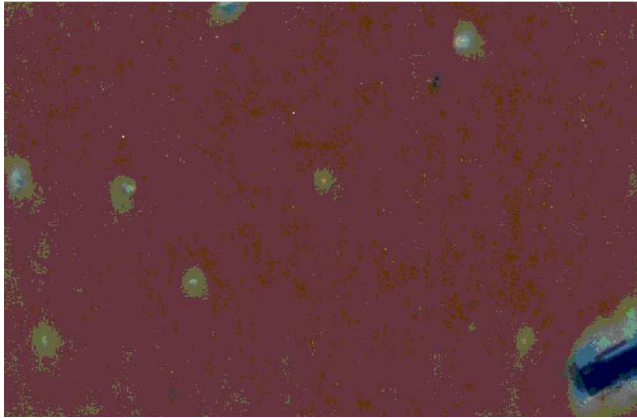
Figure 1. (Continued).

6. Experimental results

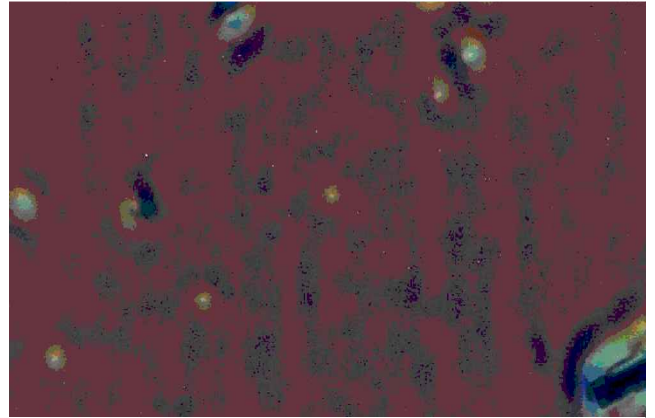
Figure 1 shows the photomicrographs obtained using the set-up described above. The times given indicate the time after the voltage was reduced that the picture was taken. The pictures start with the TP texture, as the H texture is black. Because the TP state is homogeneous, the transition from the H state to the TP state must be

accomplished through a one-dimensional relaxation. This is, as the system transforms from the H state to the TP state, the director configuration must be identical at all points in the plane of the sample.

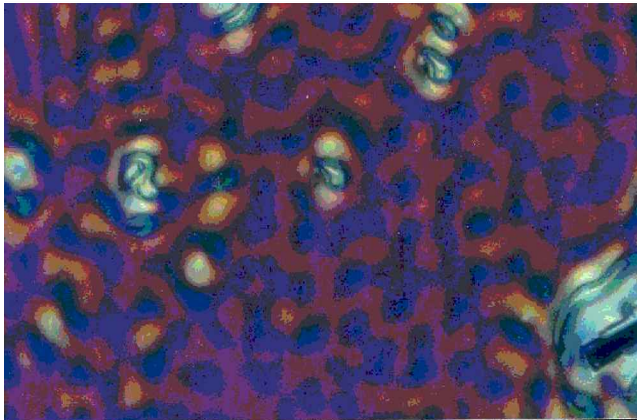
At all bias voltages except 4.5 V and 5 V, the transition from the TP state to the final state (either the P state or the FC state) starts with a two-dimensional stripe



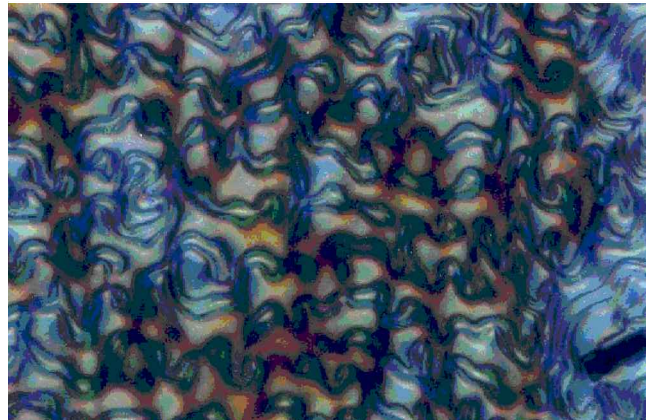
(s)



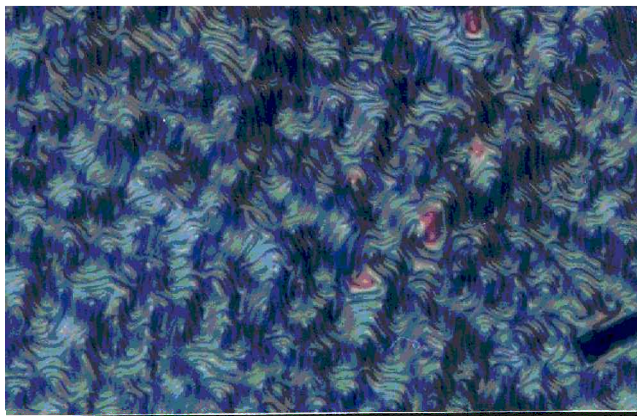
(t)



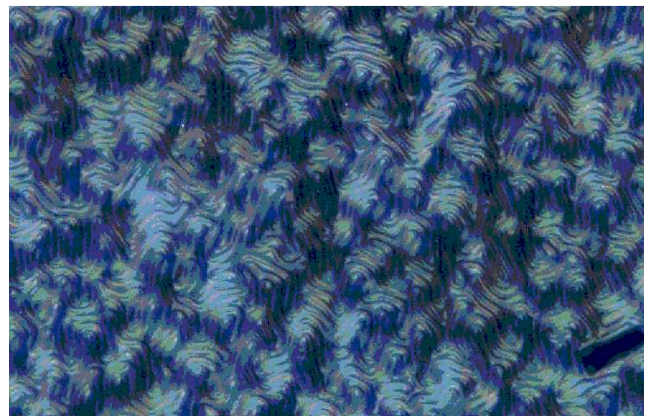
(u)



(v)



(w)



(x)

Figure 1. (Continued).

deformation. We have previously shown that for the 0 V bias this is a Helfrich–Hurault undulation distortion [5, 10]. As the texture looks practically identical for bias voltage values up to 4 V, we can assume a similar process is occurring. For the 4.5 V bias voltage case, the texture appears to be a three-dimensional Helfrich–Hurault distortion. For the 5 V case, the TP state itself is different than for 4.5 V and below, as evidenced by the change in colour. This may be because the voltage holds some of the directors homeotropic long enough for the system to insert another twist. Therefore, the TP state probably has more than one twist.

This undulation distortion increases in amplitude, after which time, through third dimensional fluctuations and further distortions, the system changes pitch and completes the transition to either the P state or the FC state, depending on the value of the bias voltage.

Figure 2 shows the experimentally measured capacitance as a function of time and bias voltage. We can see that for bias voltages below 4.5 V the curves are very similar, except that as the voltage increases the time for the capacitance to start increasing decreases. At 4.5 V, we can see that the TP state itself no longer has most of the helical axes aligned perpendicular to the glass plates, as the capacitance lower than for the other curves. This is simply because the dielectric constant associated with a field perpendicular to the long axis of the director is smaller than that associated with a field along the long axis. Thus, a lower capacitance denotes a larger pro-

portion of directors lying in the plane of the substrates. At 5 V, the TP state is almost non-existent, and the director configuration must bear little resemblance to the TP state at lower bias voltages. This is consistent with the TP state having more twists, and having fewer helical axes perpendicular to the plates at this high bias voltage.

7. Simulation results

Figures 3–7 show the calculated director configurations at various times during the relaxation for different bias voltages; we can see that all major aspects of the experiment are predicted by the simulation. The transition from the H state to the TP state is accomplished via a one-dimensional relaxation, which ‘grows’ in from the surface. We can also see that the time for the simulation transition out of the TP state decreases as the bias voltage is increased. This is shown more quantitatively in figure 8, in which there is remarkable agreement with experiment.

As these are purely two-dimensional simulations, we cannot expect good agreement after the point where the experiment shows a three-dimensional distortion, either in time or bias voltage; however, qualitative agreement with experiment can be seen even during these times. At high bias voltages the system acts very differently than at low bias voltages. We can see that for a 5 V bias, the system starts twisting in the x direction before the TP

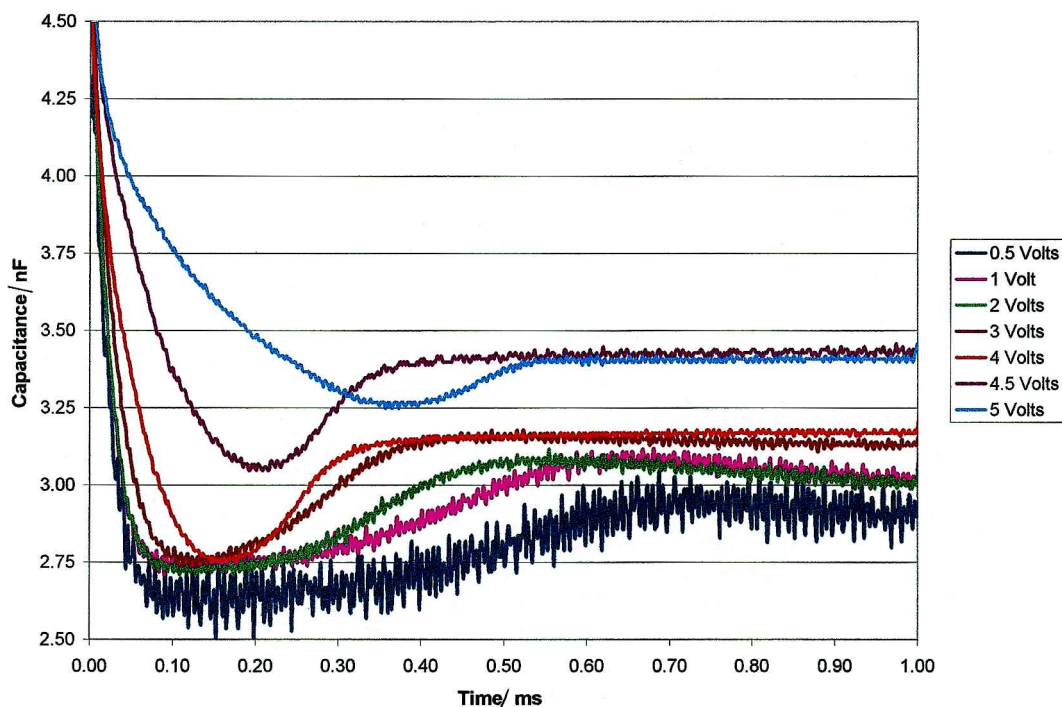
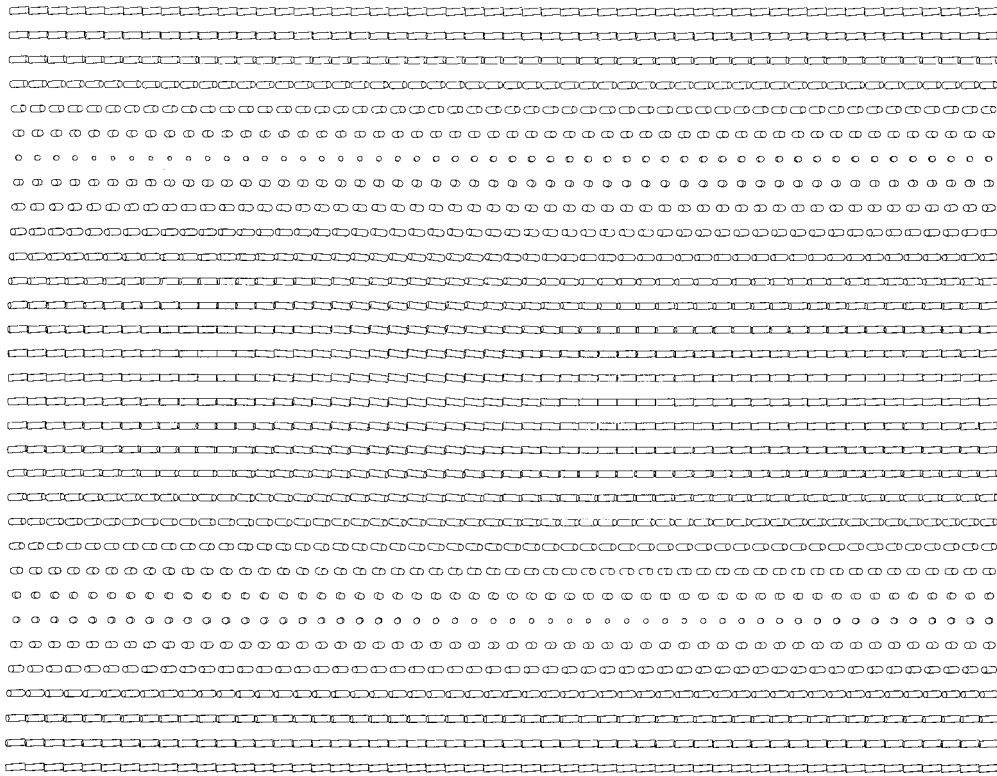
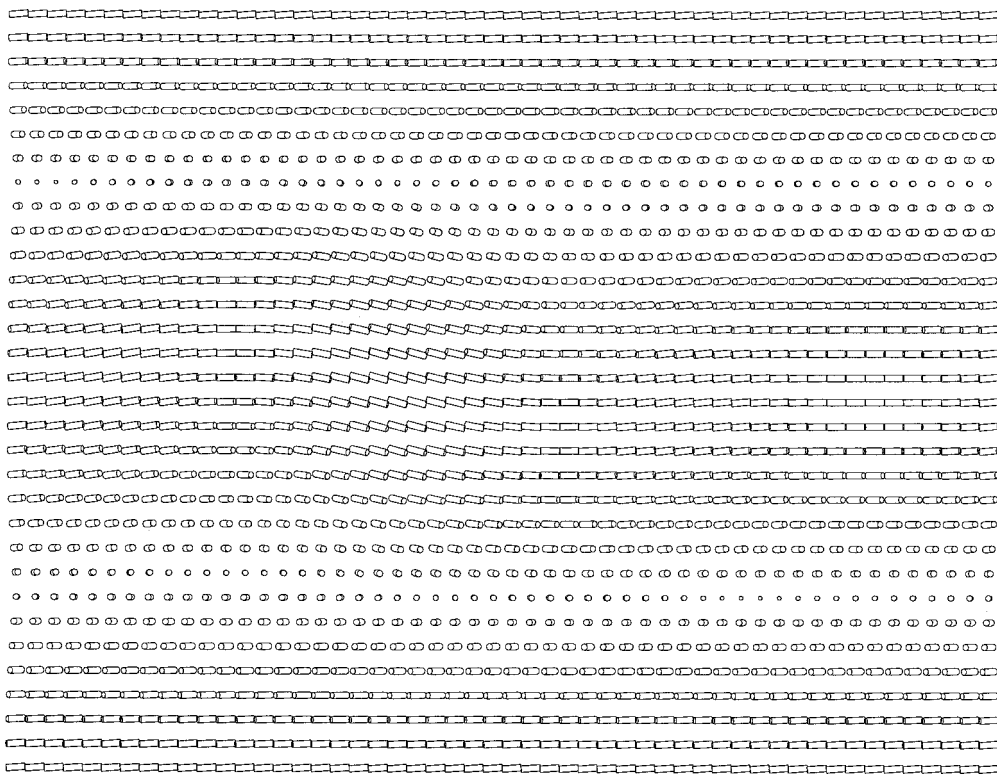


Figure 2. Measured capacitance as a function of time and bias voltage.

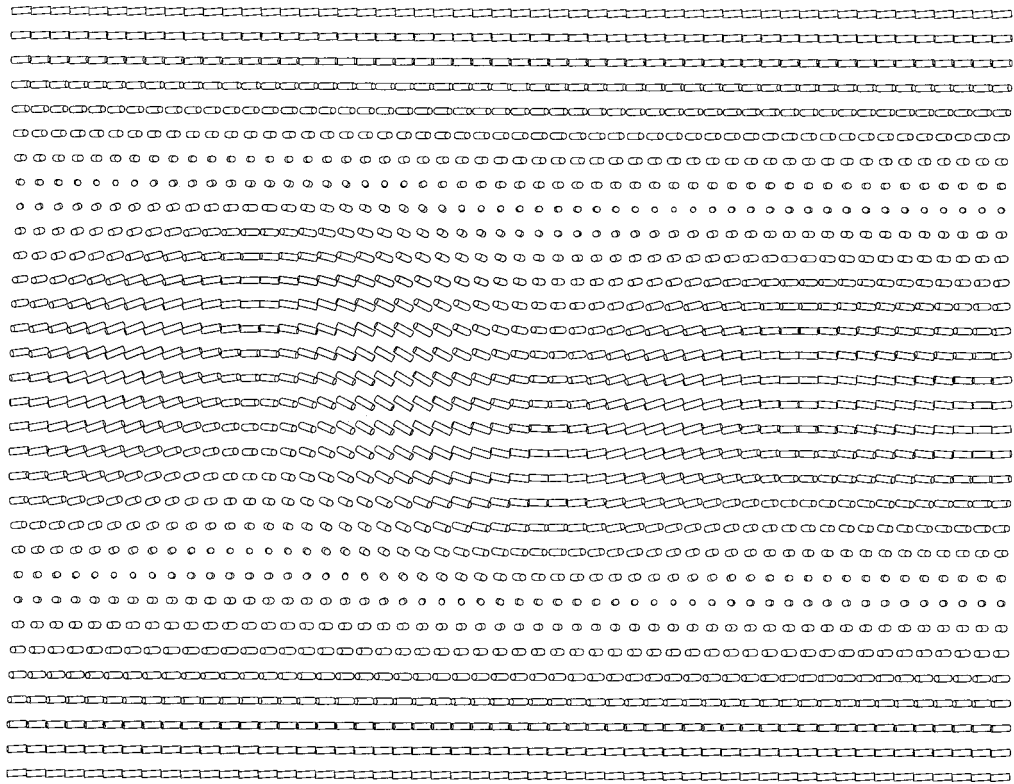


(a)

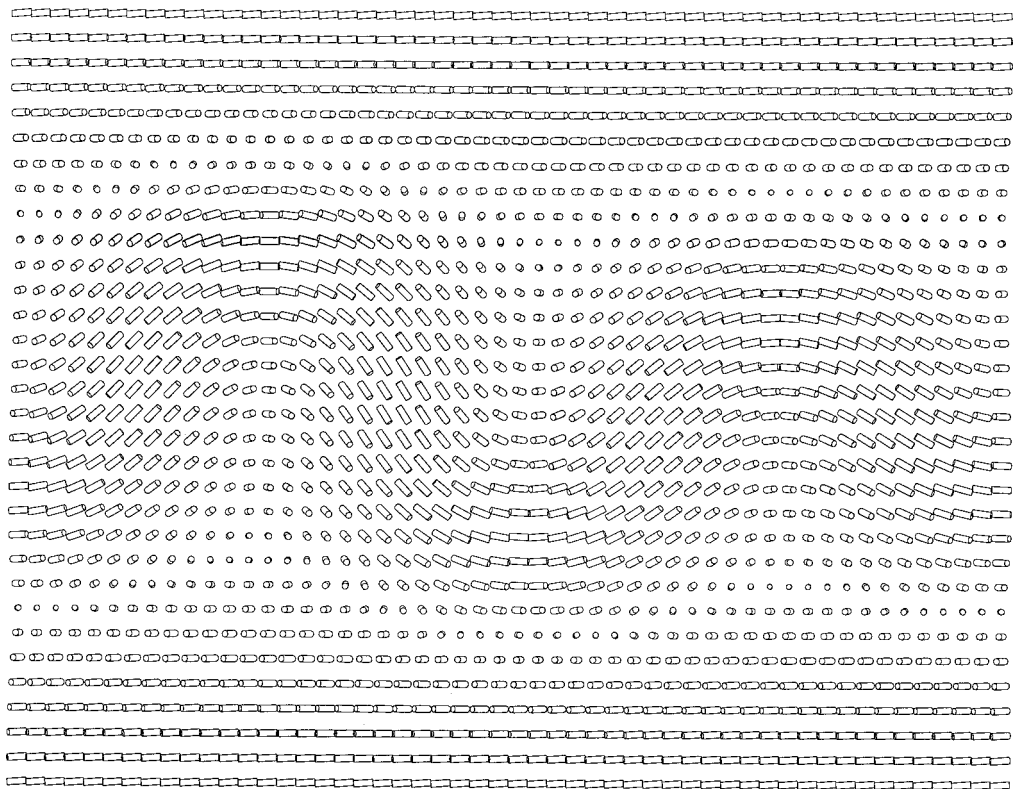


(b)

Figure 3. Simulated director configurations during the homeotropic to 0 V transition. Times are: (a) 200 ms, (b) 300 ms, (c) 400 ms, (d) 500 ms, (e) 700 ms, (f) 1000 ms.

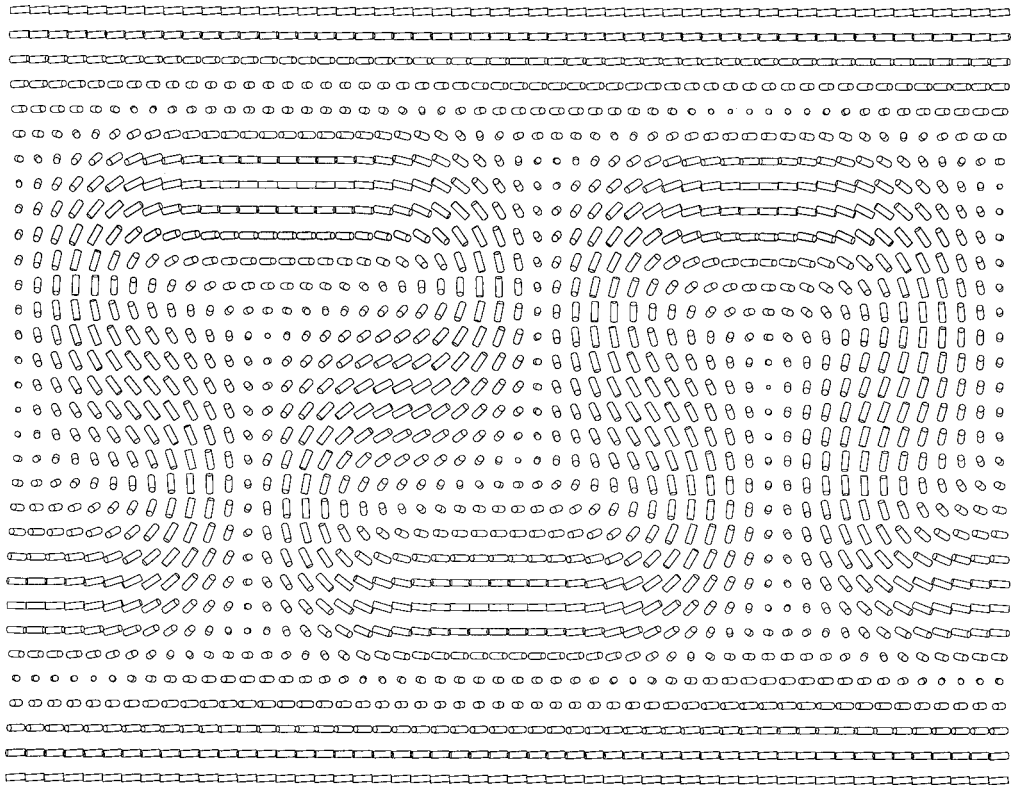


(c)

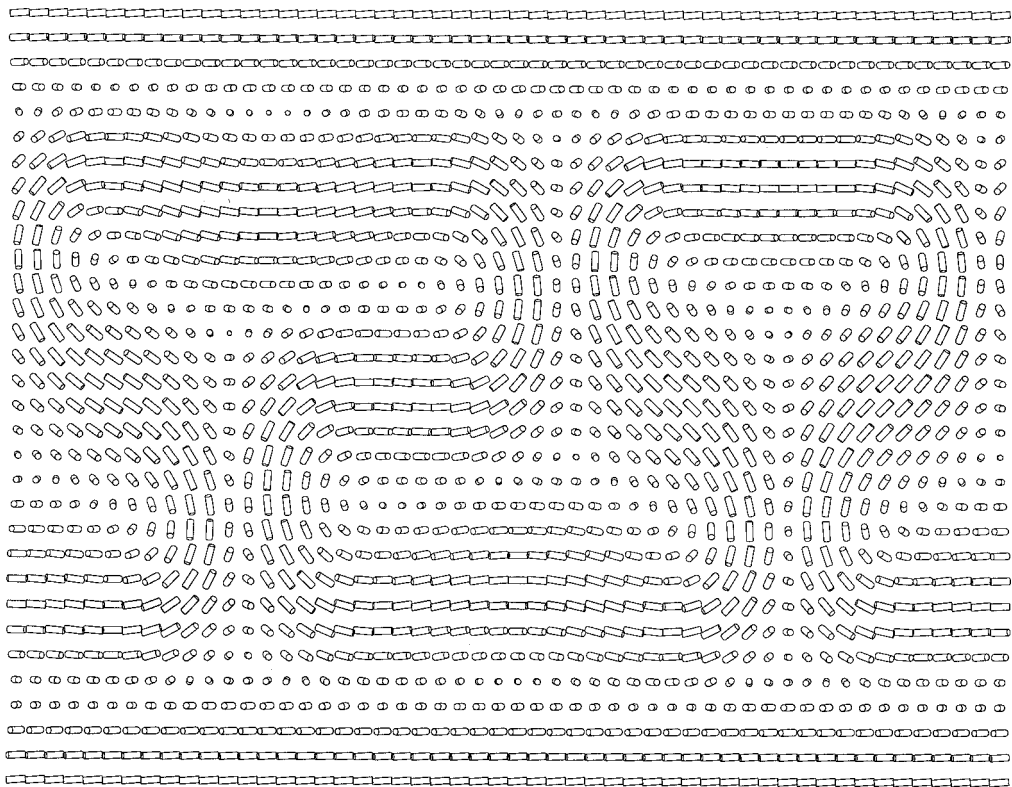


(d)

Figure 3. (Continued).



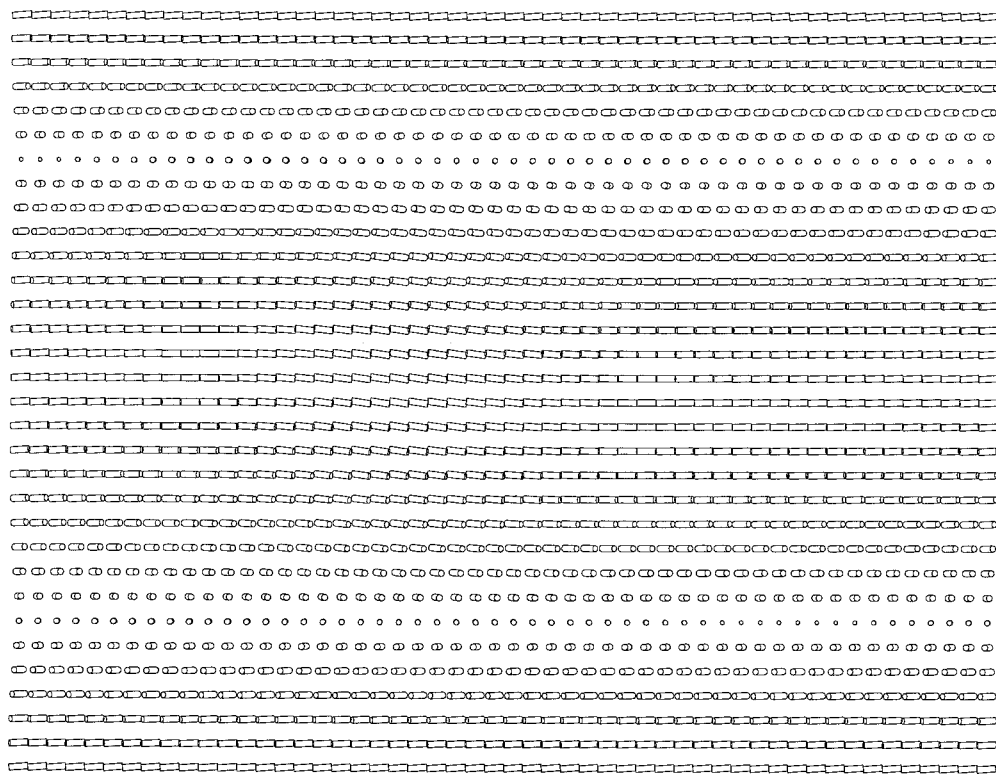
(e)



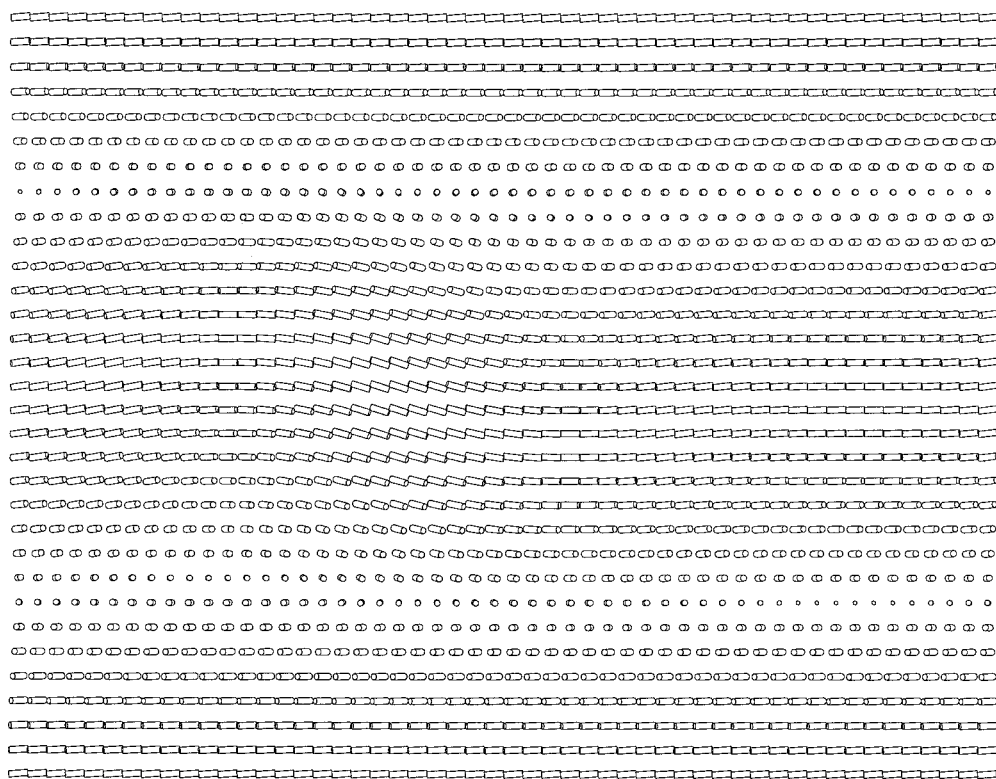
(f)

Figure 3. (Continued).

Downloaded At: 18:05 25 January 2011

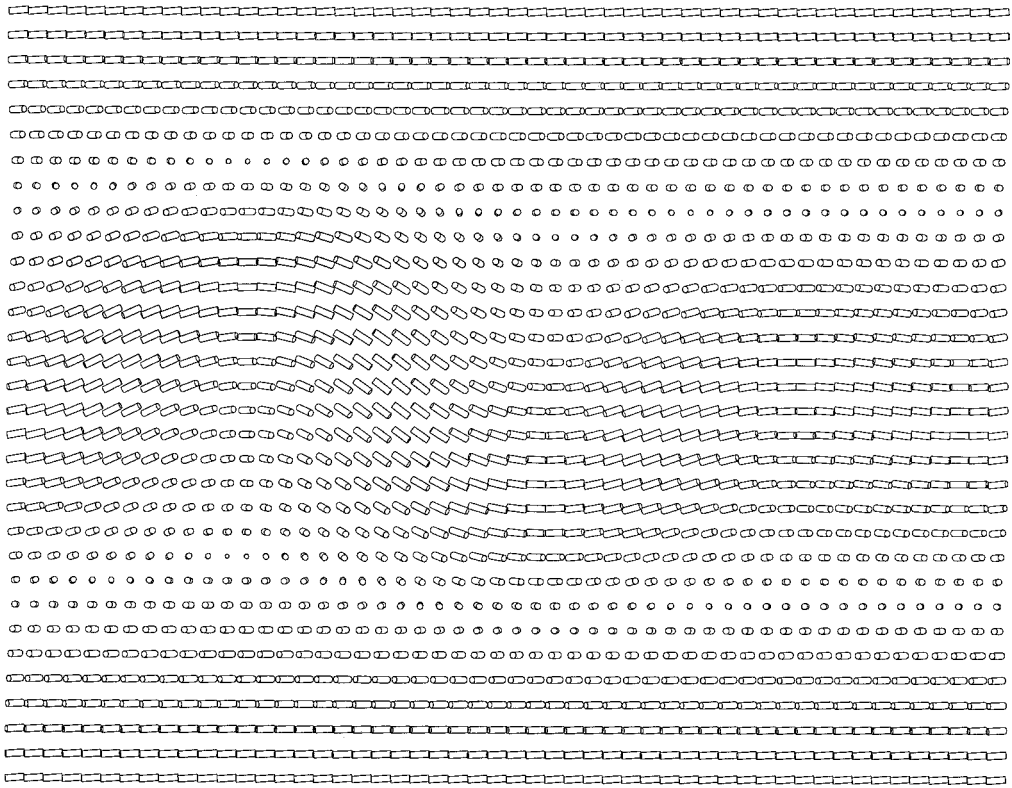


(a)

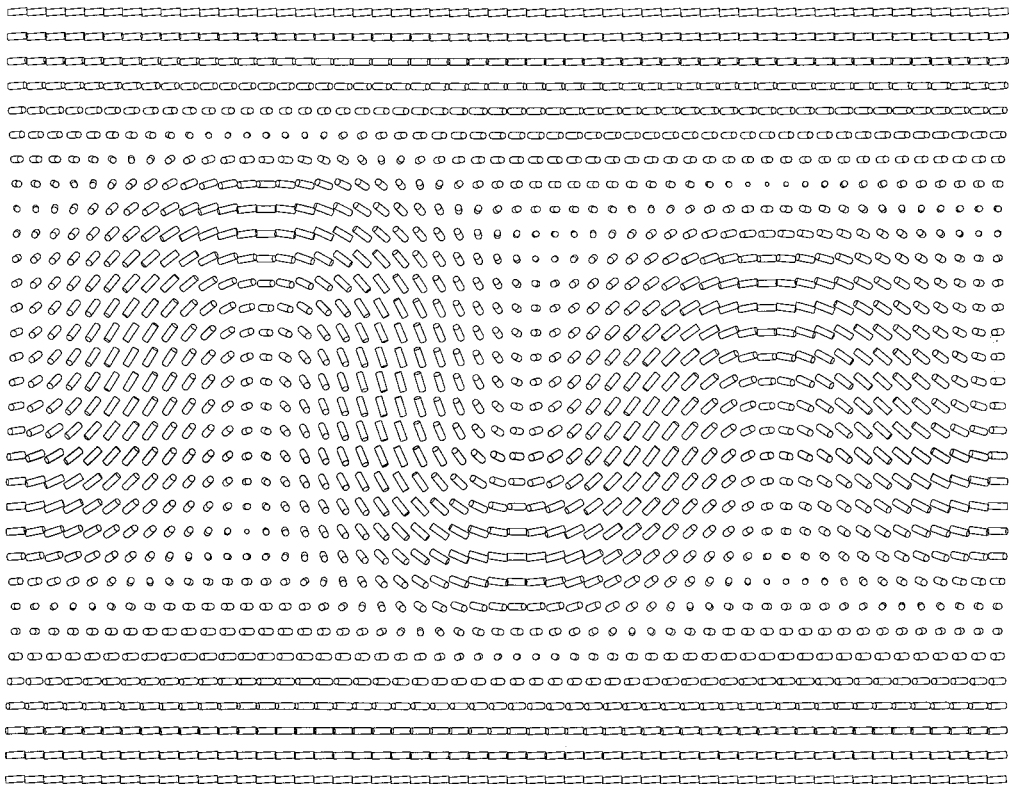


(b)

Figure 4. Simulated director configurations during the homeotropic to 2 V transition. Times are: (a) 200 ms, (b) 300 ms, (c) 400 ms, (d) 500 ms, (e) 700 ms, (f) 1000 ms.

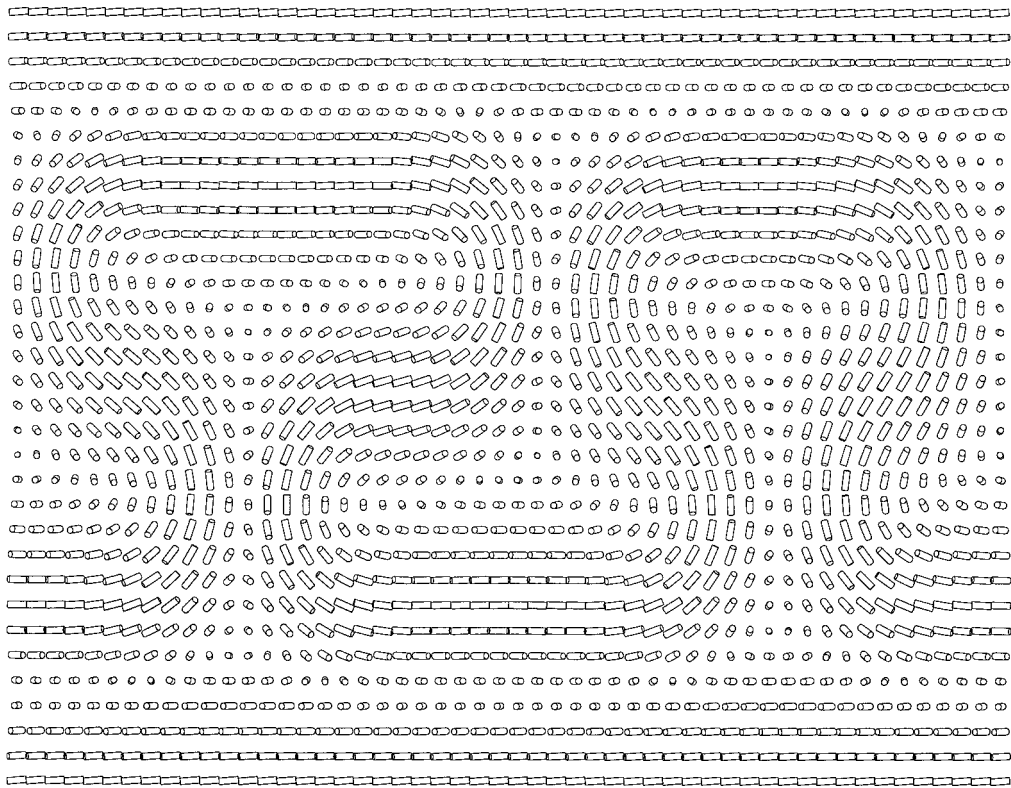


(c)

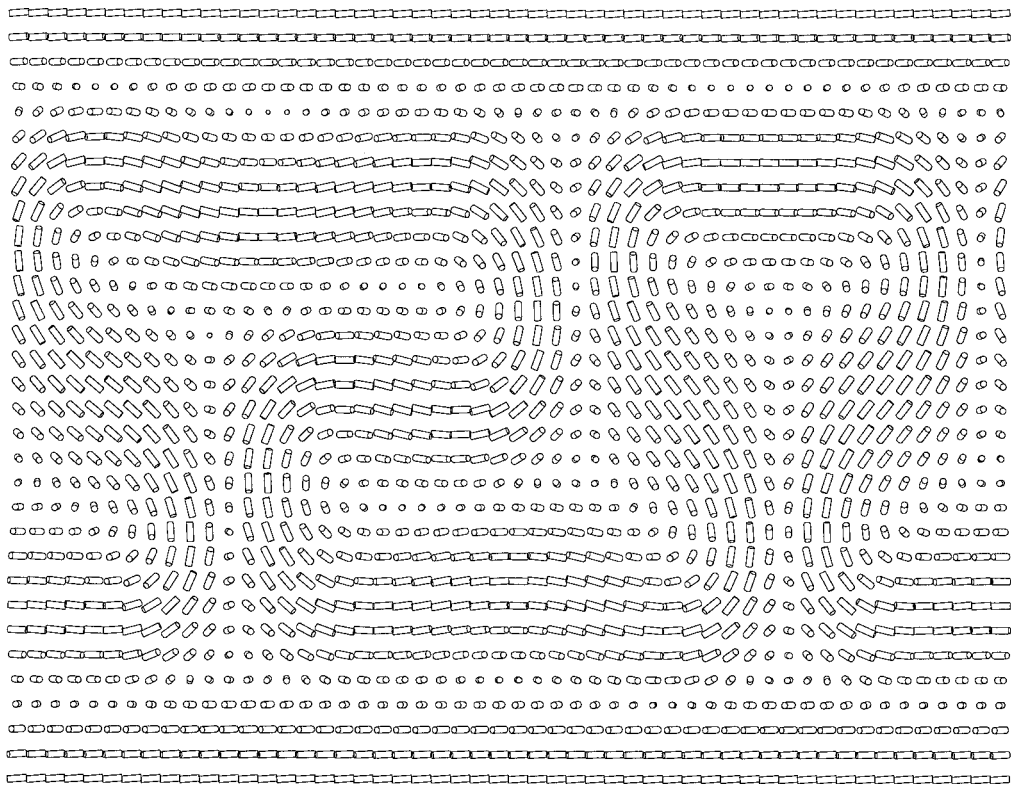


(d)

Figure 4. (Continued).

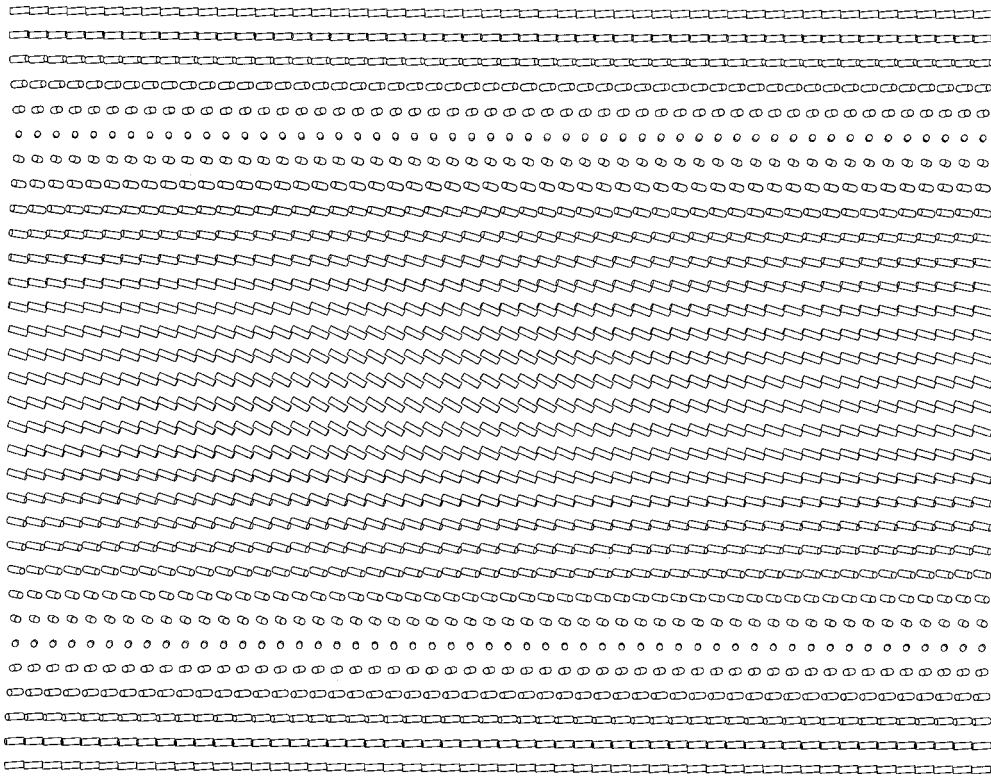


(e)

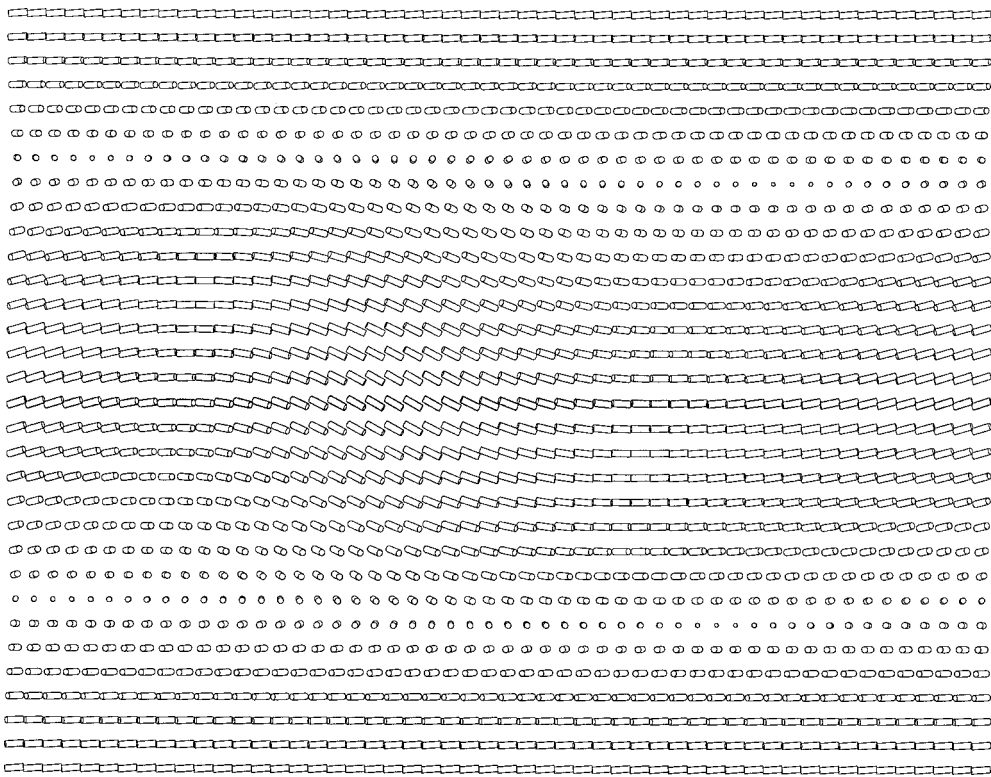


(f)

Figure 4. (Continued).

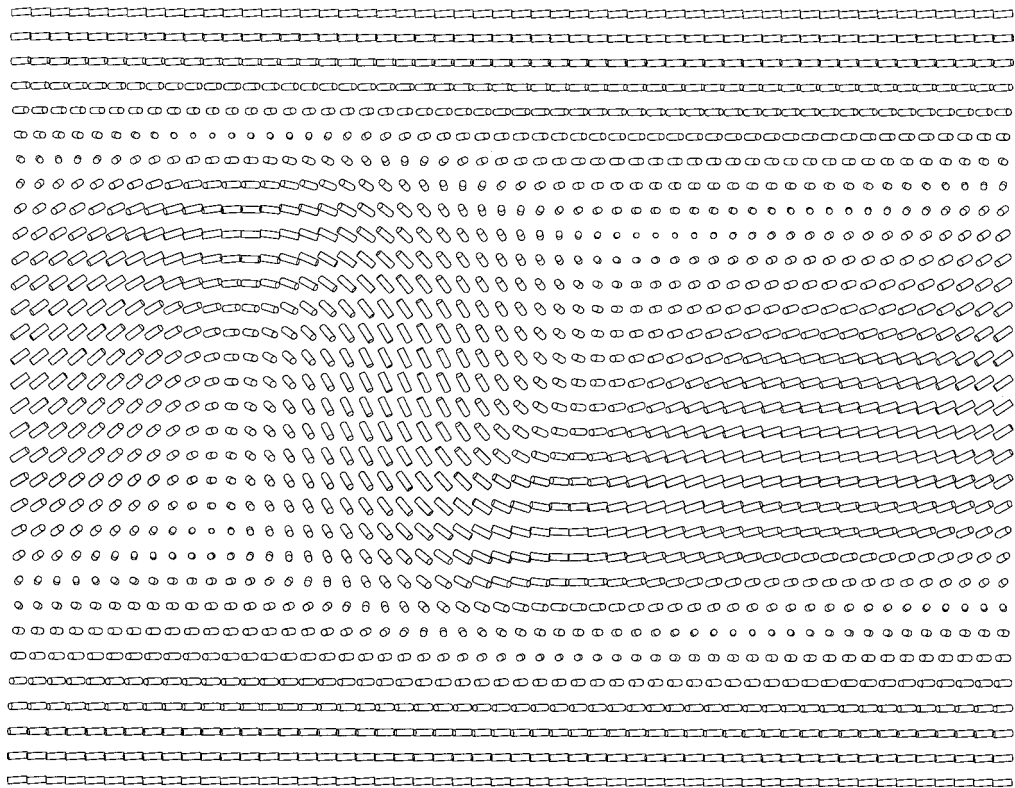


(a)

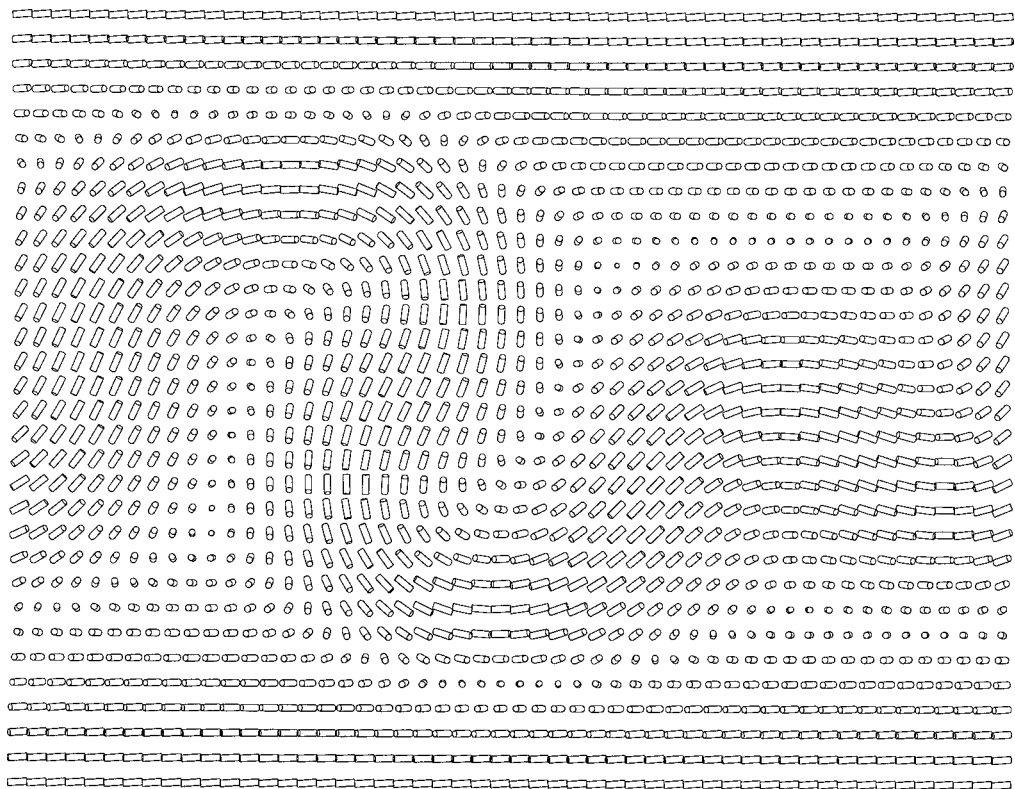


(b)

Figure 5. Simulated director configurations during the homeotropic to 4 V transition. Times are: (a) 200 ms, (b) 300 ms, (c) 400 ms, (d) 500 ms, (e) 700 ms, (f) 1000 ms.

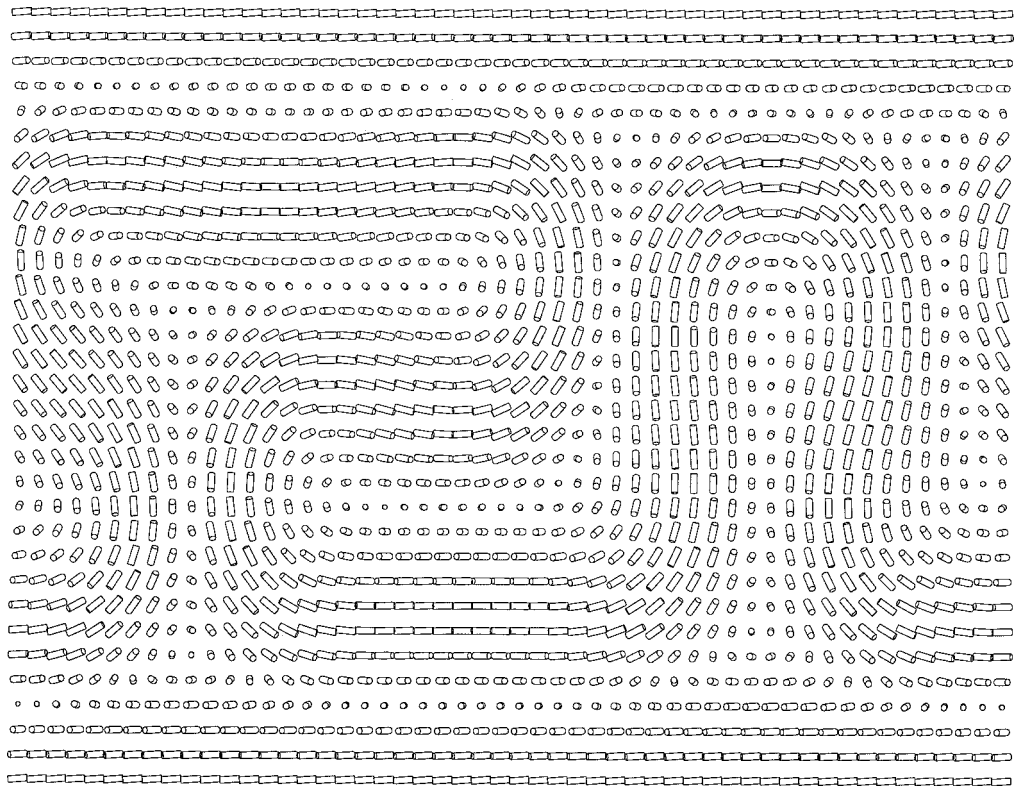


(c)

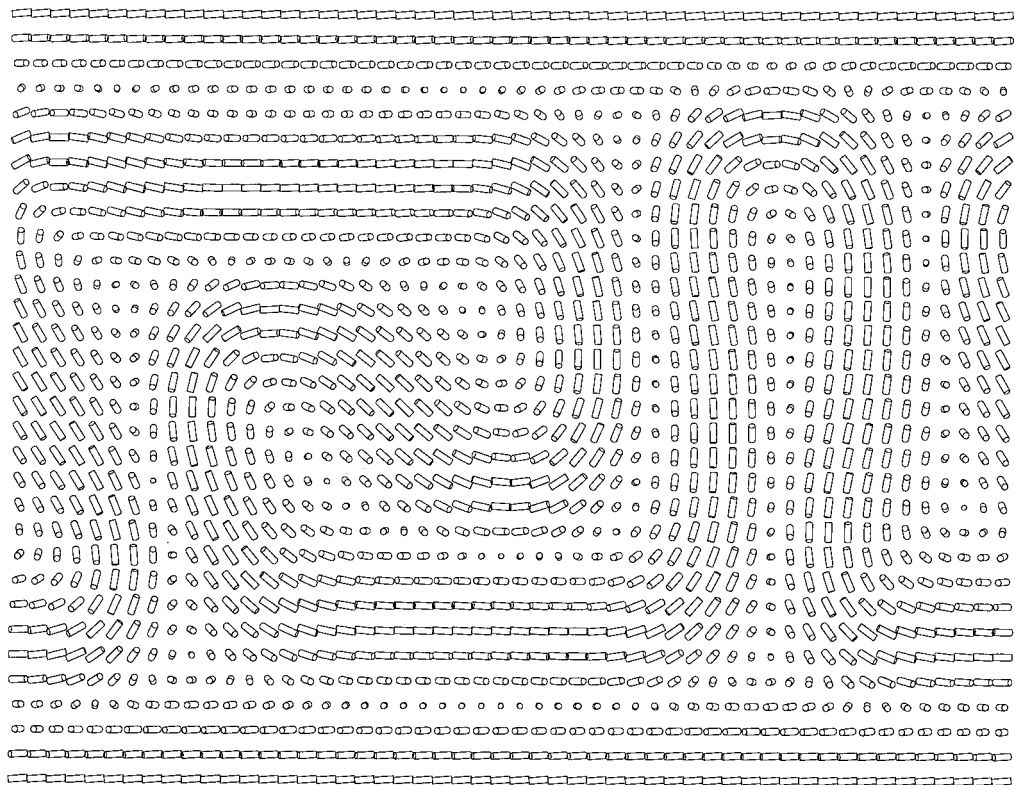


(d)

Figure 5. (Continued).



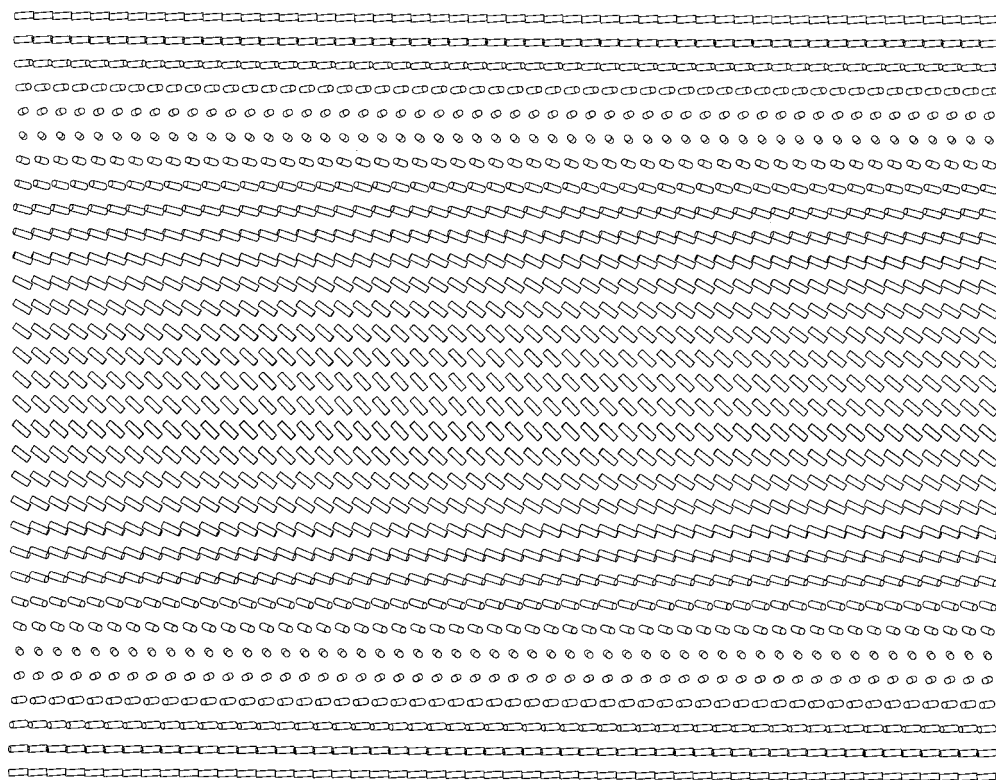
(e)



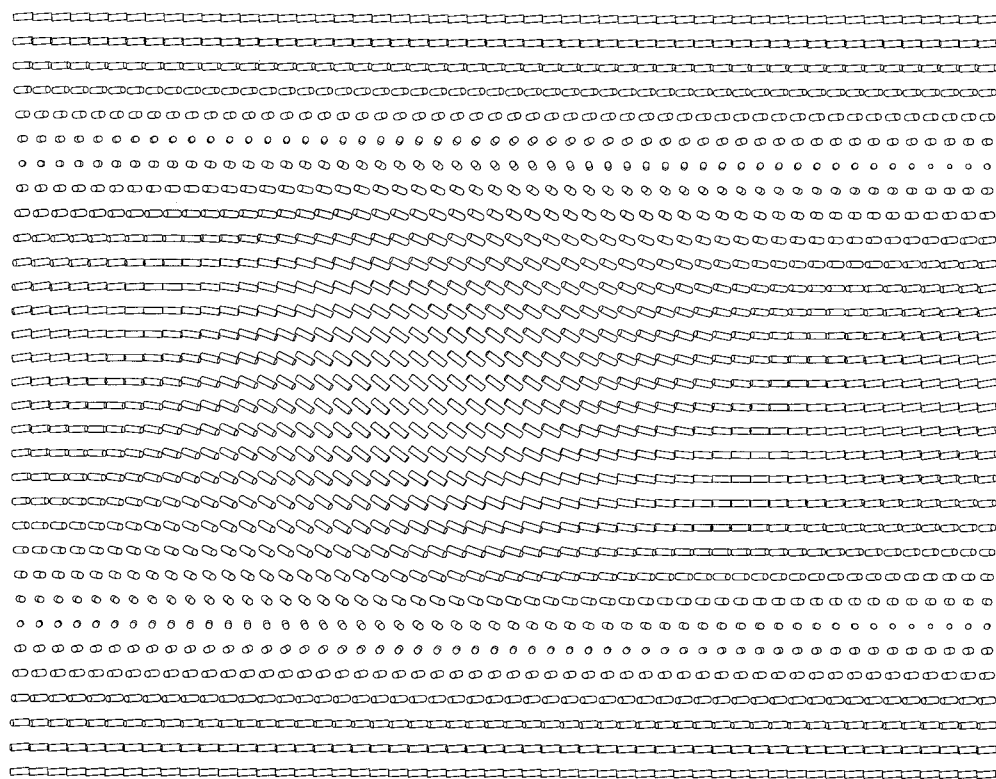
(f)

Figure 5. (Continued).

Downloaded At: 18:05 25 January 2011

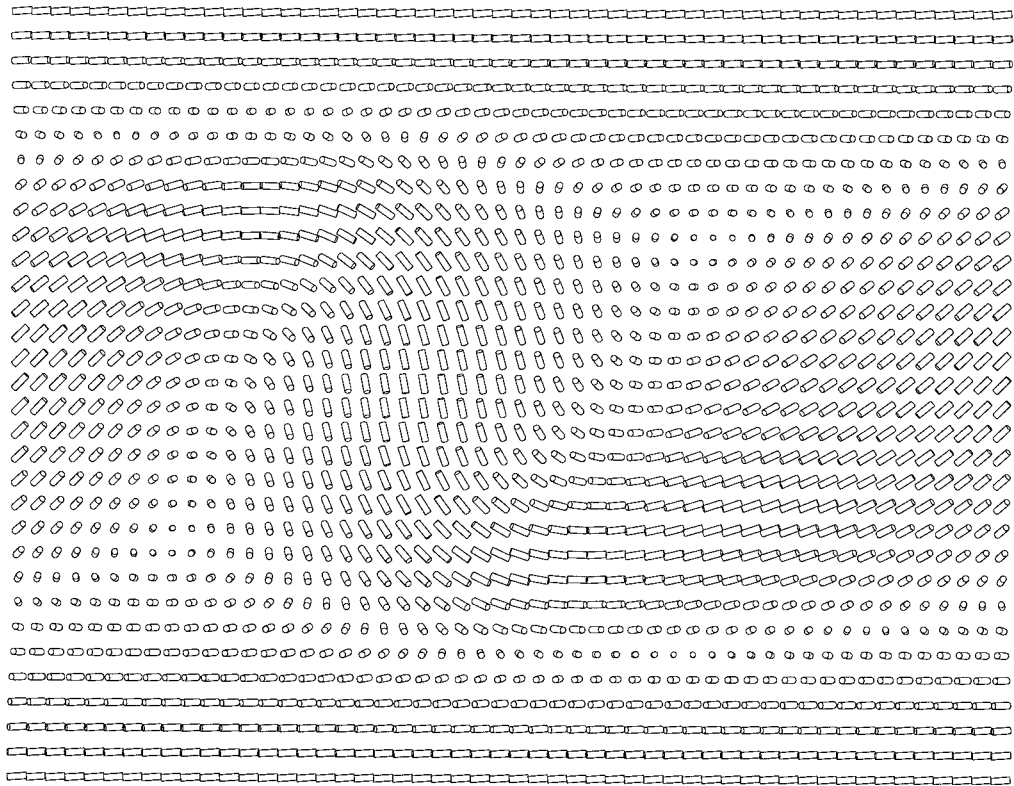


(a)

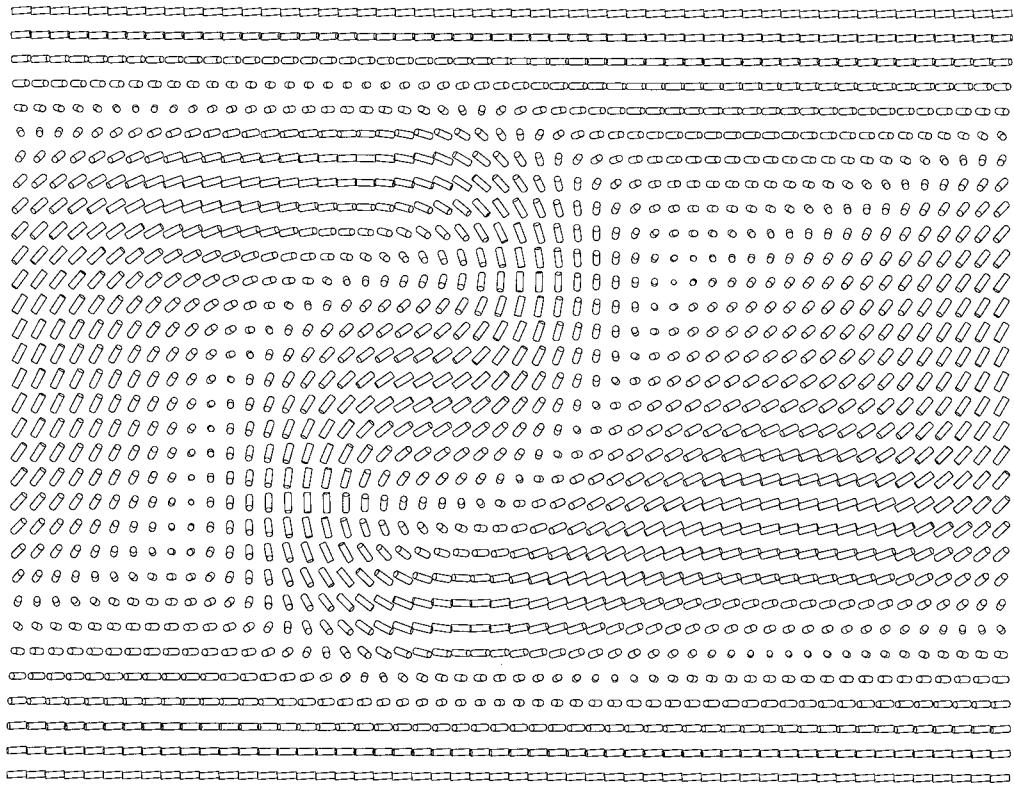


(b)

Figure 6. Simulated director configurations during the homeotropic to 4.5 V transition. Times are: (a) 200 ms, (b) 300 ms, (c) 400 ms, (d) 500 ms, (e) 700 ms, (f) 1000 ms.

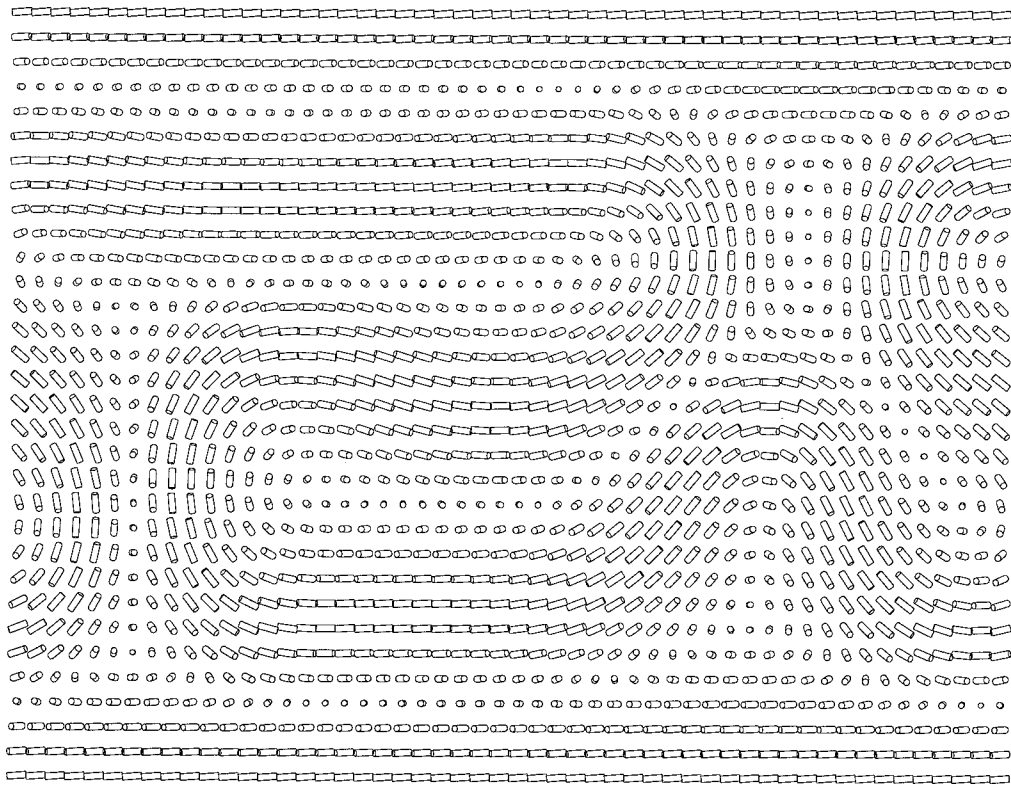


(c)

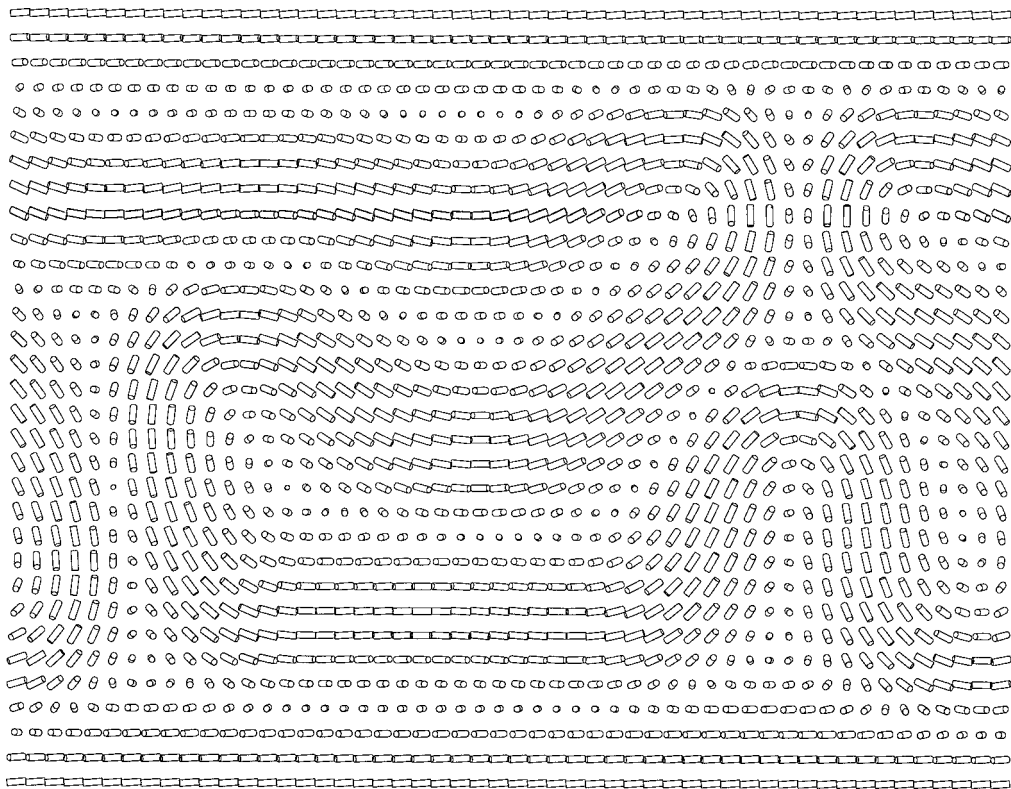


(d)

Figure 6. (Continued).

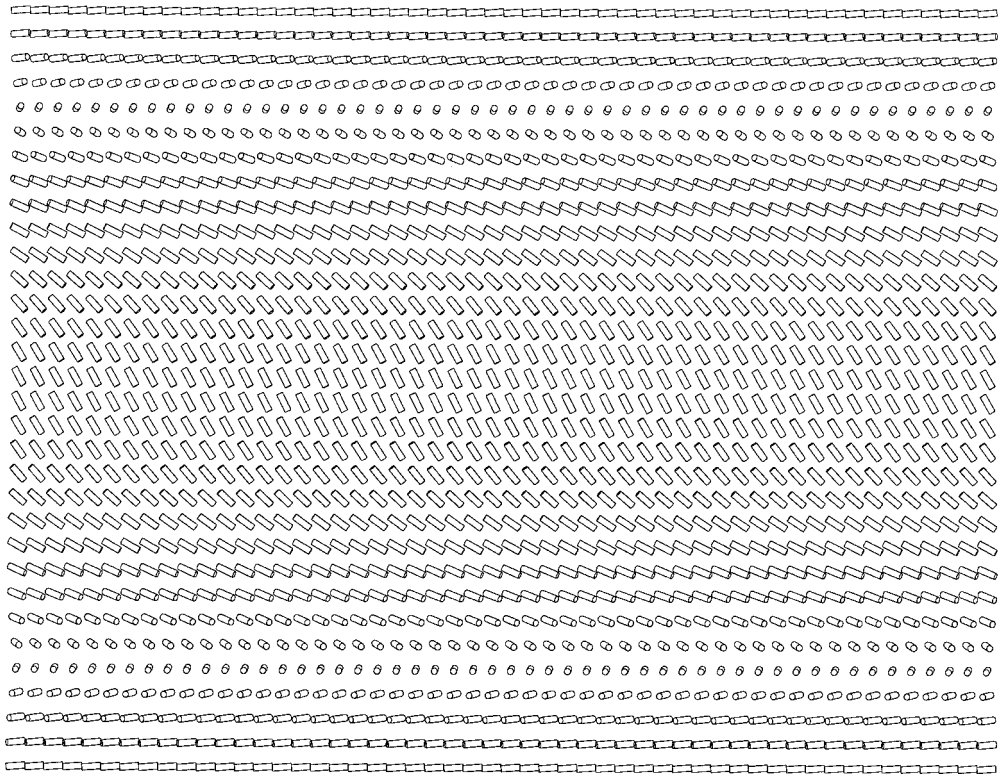


(e)

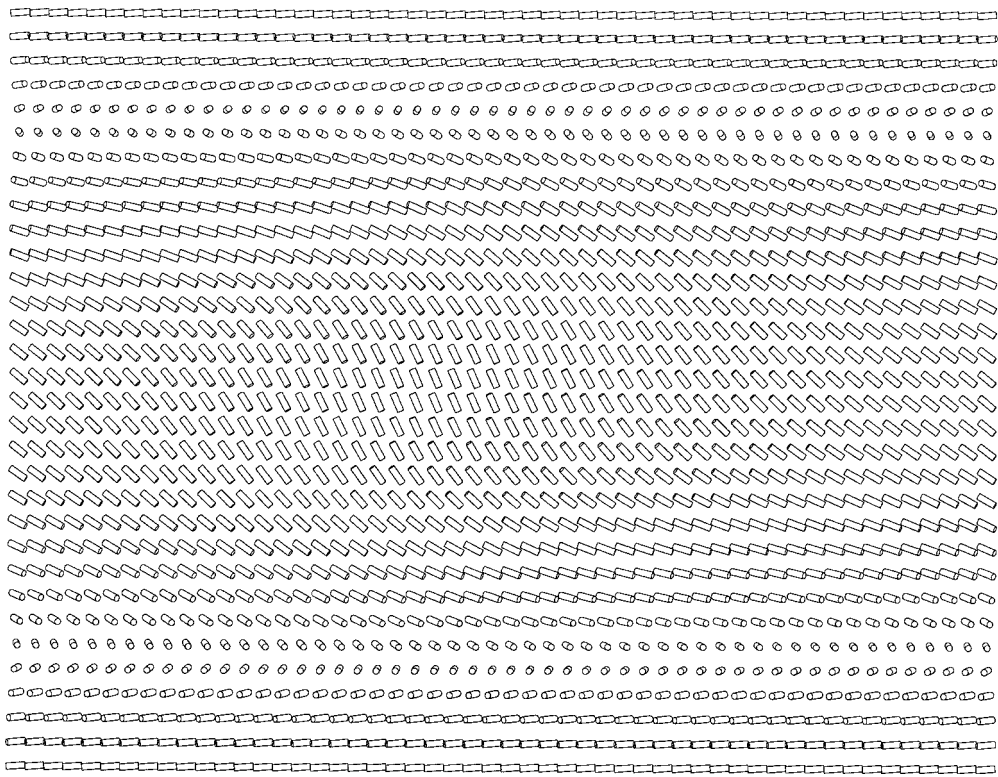


(f)

Figure 6. (Continued).

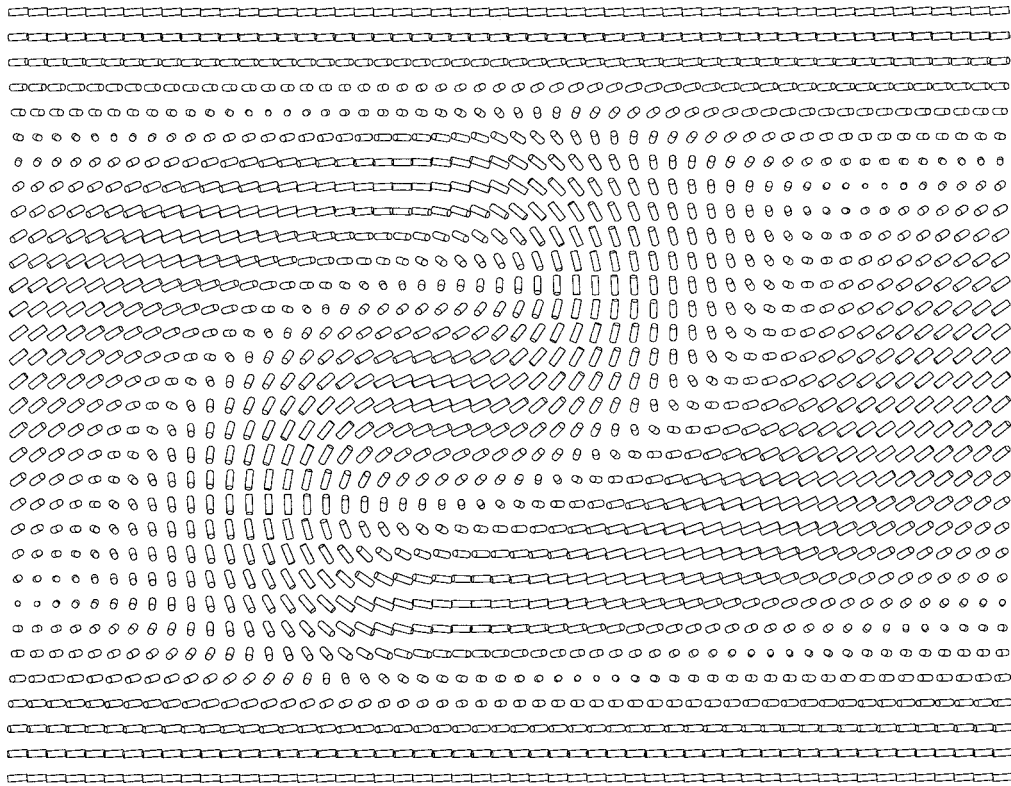


(a)

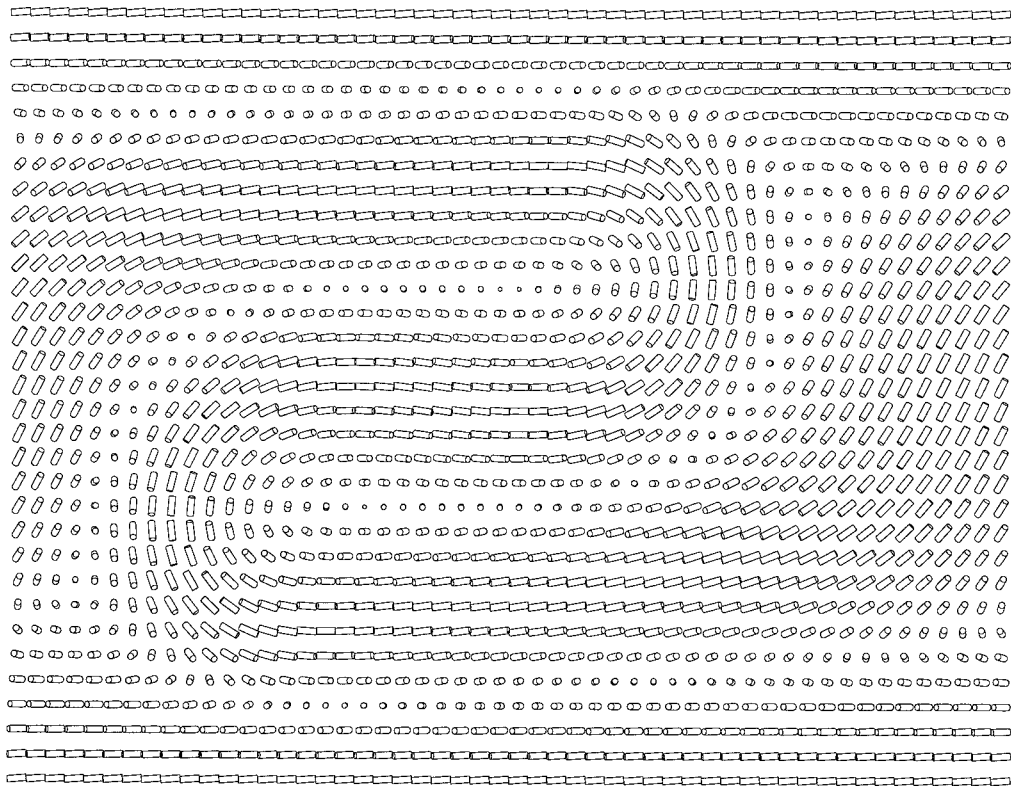


(b)

Figure 7. Simulated director configurations during the homeotropic to 5 V transition. Times are: (a) 200 ms, (b) 300 ms, (c) 400 ms, (d) 500 ms, (e) 700 ms, (f) 1000 ms.

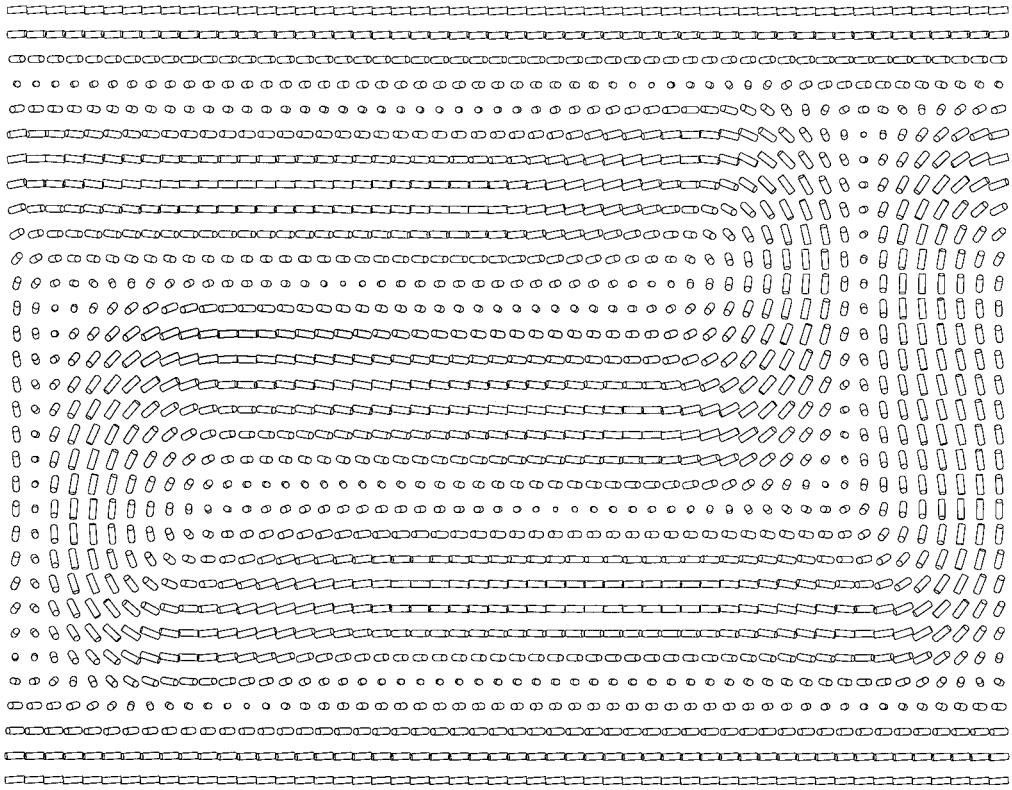


(c)

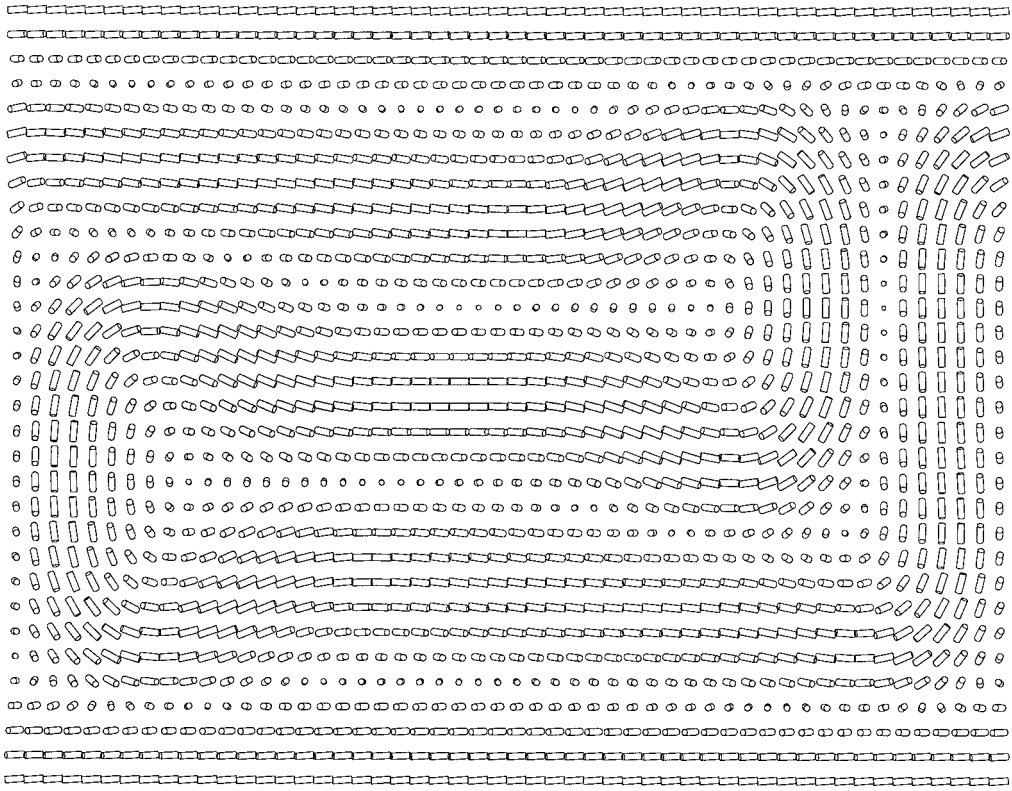


(d)

Figure 7. (Continued).



(e)



(f)

Figure 7. (Continued).

Downloaded At: 18:05 25 January 2011

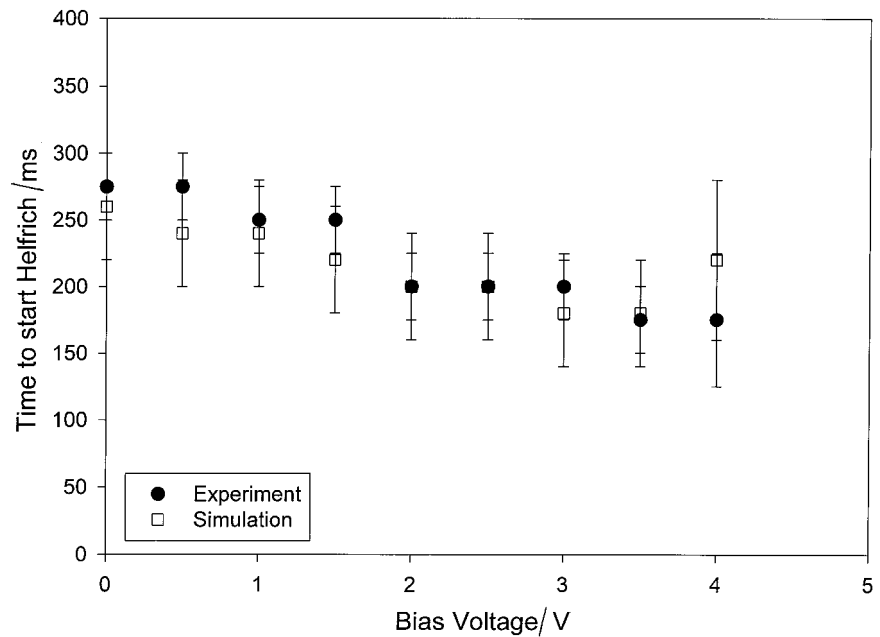


Figure 8. Measured and simulated time to start Helfrich–Hurault undulation distortion.

state fully forms; also, the TP state has two twists, instead of just the one twist of the lower bias voltages.

Figure 9 shows the calculated effective dielectric constant as a function of time and bias voltage: again there is very good agreement with experiment. All the major aspects of the experiment are predicted by the model when the third dimension is negligible. As expected, when the third dimension is significant, at higher bias voltages and later times, the agreement suffers.

8. Speed improvements

Now that we have an understanding of how the system transforms from the homeotropic state, we can suggest ways of decreasing the time required. From the

experimental photomicrographs in figure 1 it can be seen that the transition to the P state is much faster near a spacer or surface imperfection. In fact, in these regions, the system appears to miss the TP state altogether. Because this happens around every spacer seen in figure 1, we can say that the transition could be speeded up by the introduction of more spacers or surface irregularities. A more precise way to speed the transition may be to introduce polymer walls [14].

A second speed improvement can be seen in figure 8. As the bias voltage was increased, the time for the Helfrich–Hurault undulation distortion to begin was decreased. Therefore, if a drive waveform was used that held the system at a bias voltage just long enough to

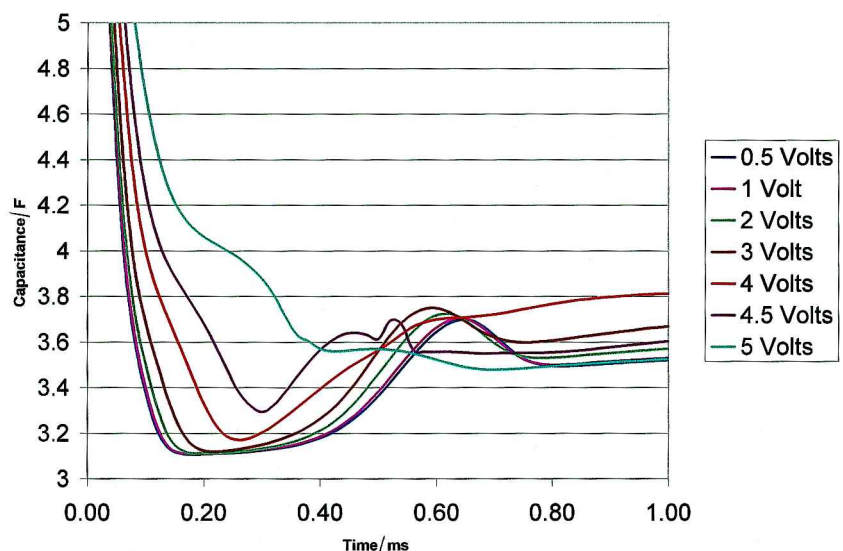


Figure 9. Calculated capacitance as a function of time and bias voltage.

initiate the distortion, and then removed, the system should transform to the P state faster.

The third and final speed improvement can be seen at the highest bias voltages, where we see the TP state having more than one twist. It may be possible to set up a waveform in such a way that it keeps the system at a high enough bias voltage to miss the TP state. It might also be possible to force the system into a TP state having so many twists that there is no longer enough twist energy to start the undulation distortion. If that state was then made to have the desired pitch, the system could be very fast indeed. In experiment, we were unable to force the system into a TP state that had more than one twist, and was stable with time. However, this may be possible for systems with higher d/P ratios.

9. Conclusion

By using a multi-dimensional simulation program and comparing the results with photomicrographs and capacitance data of the transitions, we have been able to suggest actual director level models of the transitions from the homeotropic state. These include the transition from homeotropic to transient planar to planar states, from homeotropic to transient planar to focal conic to planar states, and from homeotropic straight to focal conic.

This work was supported under NSF ALCOM grant DMR 89-20147, and DARPA grant N61331-96-C-0042.

References

- [1] DE GENNES, P. G., and PROST, J., 1993, *The Physics of Liquid Crystals*, 2nd Edn (Oxford: Oxford Science Publications).
- [2] YANG, D.-K., WEST, J. L., CHIEN, L.-C., and COANE, J. W., 1994, *J. appl. Phys.*, **76**, 1331.
- [3] LU, M.-H., 1997, *J. appl. Phys.*, **81**, 1063.
- [4] YANG, D.-K., and LU, Z.-J., 1995, *SID Dig. tech. Pap.*, **XXVI**, 351.
- [5] WATSON, P., ANDERSON, J. E., and BOS, P. J., 2000, *Liq. Cryst.* (in the press).
- [6] HAAS, G., WOHLER, H., FRITSCH, M., and MLYNSKI, D., 1993, *Mol. Cryst. liq. Cryst.*, **198**, 15.
- [7] DICKMANN, S., ESCHLER, J., COSSALTER, O., and MLYNSKI, D. A., 1993, *SID Dig. tech. Pap.*, **XXIV**, 638.
- [8] LIEN, A., CHEN, C.-J., and CHEN, 1996, *SID Dig. tech. Pap.*, **XXVII**, 175.
- [9] MORI, H., GARTLAND JR., E. C., KELLY, J. R., and BOS, P. J., 1999, *Jpn. J. appl. Phys.*, **38**, 135.
- [10] WATSON, P., ANDERSON, J. E., and BOS, P. J., 2000, *Phys. Rev. E* (in the press).
- [11] ANDERSON, J. W., WATSON, P., ERNST, T., and BOS, P. J., 2000, *Phys. Rev. E*, **61**, 3951.
- [12] See liquid crystal data sheet from E. M. Industries, USA.
- [13] HUANG, X.-Y., 1996, PhD thesis, Kent State University, USA
- [14] HOKE, C., and BOS, P., 2000, *J. appl. Phys.* (in the press).